Master's thesis

Nanofiltration and gas separation membrane fabrication using layer by layer assembly of polyelectrolytes

Author

Alula Selomon Embaye

Supervisor

Dr. Md. Mushfequr Rahman

Helmholtz-Zentrum Hereon, Germany

June 28, 2021

Abstract

Layer by layer (LBL) assembly of polyelectrolyte is a simple and versatile approach to fabricate functional membranes with good control in membrane properties such as thickness. In this study, microporous polyacrylonitrile (PAN) support membrane was modified with weak polyelectrolyte multilayer (PEM) system consisting of poly(allylamine hydrochloride) (PAH) and poly(acrylic acid) (PAA). In order to optimize the conditions for PEM coating process, the pristine PAN membrane was first surface modified via alkaline (NaOH solution) hydrolysis to generate negative surface charge to improve the adhesion of the first layer. Next, the hydrolyzed polyacrylonitrile (HPAN) support was modified with PAH and PAA polyelectrolytes by varying their assembly pH to tune the morphology and performance properties of the multilayer membrane. The membranes were characterized by SEM, streaming zeta potential, and water contact angle measurements. It was found that the pH of the coating solutions substantially influenced the morphology and performance of the polyelectrolyte multilayer membranes (PEMMs): a uniformly dense and thin film was observed at PAH/PAA solution pH (6.5/6.5) due to the high intrinsic charge compensation occurring between the two PEs since both PEs are nearly fully ionized at pH 6.5. Likewise, a thin but less dense film was obtained at PAH/PAA solution pH (2.5/8.5) where both PEs are fully ionized. On the other hand, the thickest layer was formed at PAH/PAA solution pH (2.5/4.5) combinations where PAA is only partially charged and PAH is fully charged. The PAH2.5/PAA4.5, PAH2.5/PAA8.5, and PAH6.5/PAA6.5 demonstrated a pure water permeance of 35.2 8.72, and 2.34 L·m-2·h-1·bar-1, respectively after coating with four layers. However, the membranes showed very poor gas separation performance. Results of this study clearly demonstrate the potential of using weak PEs solution pH as a tuning parameter to prepare PEMMs for specific applications.

Key words: Polyelectrolyte, layer by layer assembly, polyelectrolyte multilayer membrane (PEMM), poly(allylamine hydrochloride) (PAH), and poly(acrylic acid) (PAA)

Resumen

El ensamblaje capa a capa (LBL) de polielectrolitos es un método sencillo y versátil para fabricar membranas con grupos funcionales, que permitan un buen control de las propiedades de la membrana como el grosor. En este estudio, se modificó la membrana de soporte de poliacrilonitrilo (PAN) microporoso con un sistema de multicapas de polielectrolitos débiles (PEM) compuesto por clorhidrato de poli(alilamina) (PAH) y poli(ácido acrílico) (PAA). Para optimizar las condiciones del proceso de recubrimiento PEM, la membrana de soporte PAN fue modificada primero superficialmente mediante hidrólisis alcalina (solución de NaOH), para generar una carga superficial negativa con el fin de mejorar la adhesión de la primera capa. A continuación, el soporte de poliacrilonitrilo hidrolizado (HPAN) fue modificado con polielectrolitos PAH y PAA variando su pH durante el ensamblaje para ajustar la morfología y el rendimiento de la membrana multicapa. Las membranas fueron caracterizadas mediante SEM, potencial zeta de flujo y mediciones del ángulo de contacto (agua). El pH de las soluciones de recubrimiento influyó significativamente en la morfología y el rendimiento de las membranas multicapa de polielectrolitos (PEMM): se observó una película uniformemente densa y fina a un valor de pH de solución de PAH/PAA (6,5/6,5) debido a la elevada compensación de carga intrínseca que se produce entre los dos PE, puesto que ambos PE estuvieron casi completamente ionizados a un pH de 6,5. Asimismo, se obtuvo una película delgada, pero menos densa, a un pH de la solución de PAH/PAA (2,5/8,5) en el que ambos PE estuvieron totalmente ionizados. Por otro lado, la capa más gruesa fue sintetizada mediante las combinaciones de pH de la solución PAH/PAA (2,5/4,5), donde el PAA estuvo parcialmente cargado y el PAH totalmente cargado. Los valores de permeabilidad de agua pura para las membranas PAH2.5/PAA4.5, PAH2.5/PAA8.5 y PAH6.5/PAA6.5 fueron 35,2 8,72 y 2,34 L-m-2-h-1-bar-1, respectivamente, tras el recubrimiento con cuatro capas. Sin embargo, el rendimiento de las membranas en la separación de gases fue muy bajo. Los resultados de este estudio demuestran claramente el potencial de utilizar el pH de la solución de PEs débiles como parámetro de ajuste para preparar PEMMs para aplicaciones específicas.

Palabras clave: polielectrolitos, ensamblaje capa a capa (LBL), membranas multicapa de polielectrolitos (PEMM), por clorhidrato de poli(alilamina) (PAH), y poli(ácido acrílico) (PAA)

Acknowledgment

First of all, I would like to express my sincere gratitude and thankfulness to my promotor Dr. Md. Mushfequr Rahman for offering me such a prodigious opportunity to undertake my master thesis in his Materials chemistry and mass transfer (PMC) group at Helmholtz Hereon. Working with him was a great privilege thanks to his continuous supervision, invaluable advises, significant concern and great patient. Thanks a lot, promotor Dr. Md. Mushfequr!

I would like also to thank all colleagues in the Materials chemistry and mass transfer (PMC) group for their continuous guidance and support throughout the experimental work. Their cooperation, kindness, and patience during the work endow me to learn a lot. I will always indebted to them for the training and guidance I got that could potentially help me to be an independent researcher in my future endeavors. During the work, I met with many colleagues for whom I have great respect and thankfulness and I wish to express my warmest gratitude to all who have assisted me with my thesis work at Helmholtz Hereon.

My thanks and appreciation also goes to the Instrumental Structure Analysis team members and particularly to Dr. Martin Held for sharing me their precious time to characterize the membranes. Last but not least, the EM3E-4SW education program is the one that revolutionized and transformed my life, where I learned and acquired innumerable knowledge and skills from this multidisciplinary program. The financial support from Erasmus Mundus is momentously accredited. All professors who taught me in this program are very appreciated and respected.

Contents

Abstract ii

Acknowledgment iv

List of Figures iii

1. Introduction 1

1.1 Objectives 3

2. Literature review 3

2.1 Polyelectrolyte multilayer membrane 3

3. Experimental part 11

3.1 Material and chemicals 11

3.2 PAN membrane post modification 12

3.3 PEMM via Layer by Layer Assembly 12

3.4 Characterization of the membranes 13

3.4.1 Scanning Electron Microscopy (SEM) 14

3.4.2 Fourier Transform Infrared Spectroscopy (FTIR) 14

3.4.3 Streaming Potential Measurements 14

3.4.4. Contact Angle measurement 15

3.4.5 Gas Permeation testing 15

3.4.6 Pure water permeance measurement 16

4. Result and Discussion 16

4.1 PAN membrane hydrolysis 18

4.2 PEMM Fabrication 20

4.2.1 Single layer deposition 21

4.2.2 Second layer deposition 22

4.2.3 Third layer deposition 24

4.2.4 Fourth layer deposition 25
4.3 Membrane separation performance 26
4.3.1 Water Peremeance 26
4.3.2 Gas separation performance 27
5. Conclusion and recommendation 29
5.1. Conclusion 29
5.2 Recommendation 30
6. Refernce 31
7. Appendix 41

List of Figures

Figure 1. Thin film composite (TFC) membrane..... 2
Figure 2. LBL assembly of PEs (dip coating)..... 4
Figure 3. Intrinsic (a) and Extrinsic (b) charge compensation mechanism 6
Figure 4. Charge compensation between (a) two fully charged PEs and (b) one fully ionized and another partially charged PEs 9
Figure 6. Chemical structures of PEs used in this work. 11
Figure 7. Schematic representation - (A) Roll-to-Roll (R2R) dip coating machine developed at Institute of Membrane research, Helmholtz Zentrum Hereon and (B) cycle of multilayer buildup process, assuming negatively charged substrate..... 12
Figure 7. SEM surface image of membranes: (a) Pristine PAN, (b) PAN/PAH (c) PAN/PEI, (d) PAN/PAH dipped in water for 4 days, (e) HPAN/PAH dipped in water for 4 days, (f) Zeta potential of HPAN and the water dipped PAN/PAH and HPAN/PAH membranes. All SEM images are taken at 100kx magnification. 17
Figure 9. SEM micrographs of top surface of (a) untreated PAN and (b), (c), (d), (e) and (f) are HPAN membranes hydrolyzed under 2M NaOH alkaline solution and hydrolysis time of 1, 1.5, 2, 2.5 and 3 hr., respectively. All images are (100kx) magnification. 19
Figure 10. The FTIR spectra of pristine and alkaline hydrolyzed PAN membranes and..... 20
Figure 11. SEM image: cross section (a) and surface (b) of HPAN/PAH2.5, cross section (c) and surface (d) of HPAN/PAH6.5, and Zeta potential (e) of HPAN and the other single layered membranes prepared from 0.15 wt. % PE in 5mM NaCl salt solution..... 22
Figure 12. SEM image of PEMMs: cross section (a) and surface (b) of (PAH2.5/PAA4.5)2, cross section (c) and surface (d) of (PAH2.5/PAA8.5)2, cross section (e) and surface (f) of (PAH6.5/PAA6.5)2, and Zeta potential (g) of all membranes prepared from 0.15 wt. % PE in 5mM NaCl salt solution..... 23
Figure 13. SEM image of PEMMs: cross section (a) and surface (b) of HPAN/PAH2.5/PAA4.5/PAH2.5, cross section (c) and surface (d) of (HPAN/PAH2.5/PAA8.5/ PAH2.5, cross section (e) and surface (f) of (HPAN/PAH6.5/PAA6.5/ PAH6.5, and Zeta potential (g) of all membranes prepared from 0.15 wt. % PE in 5mM NaCl salt solution..... 24

Figure 14. SEM image of PEMMs: cross section (a) and surface (b) of HPAN/PAH2.5/PAA4.5/PAH2.5/PAA4.5, cross section (c) and surface (d) of PAH6.5/PAA6.5/ PAH6.5/PAA6.5, and Zeta potential (e) of both membranes prepared from 0.15 wt. % PE in 5mM NaCl salt solution. 25
Figure 14. Average incremental thickness contributed by a PAA and PAH adsorbed layer as function of solution pH. Both the PAH and PAA dipping solutions in this case were at the same pH. Solid line represents the PAA layer thickness, and the dashed line is the PAH[77]. 41
Figure 15. SEM (a) surface and (b) cross section image of HPAN hydrolyzed under 2M NaOH solution and hydrolysis time of 2 hours. 41
Figure 16. Water contact angle measurement of selected PEMMs prepared from different pH combinations as a function of bilayer 42

The EM3E-4SW Master is an Education Programme supported by the European Commission, the European Membrane Society (EMS), the European Membrane House (EMH), and a large international network of industrial companies, research centres and universities (www.em3e.eu). The EM3E-4SW education programme has been funded with support from the European Commission. This publication reflects the views only of the author, and the Commission cannot be held responsible for any use which may be made of the information contained therein.

El EM3E-4SW Master es un programa de educación respaldado por la Comisión Europea, la European Membrane Society (EMS), la European Membrane House (EMH) y una gran red internacional de empresas industriales, centros de investigación y universidades(www.em3e.eu).

El programa educativo EM3E-4SW ha sido financiado con el apoyo de la Comisión Europea. Esta publicación refleja solo las opiniones del autor, y la Comisión no se hace responsable del uso que pueda hacerse de la información contenida en el mismo.

1. Introduction

The rapid global population growth, industrialization, economic advancement and climate change have triggered a rising demand and constraints of fundamental commodities such as freshwater, energy, and other raw materials that are essential elements in many industries. A recent report disclosed that approximately 1.42 billion people reside in a place facing high water shortage[1], and it is projected that around 40% of the total world's population will suffer from a serious water deficit by 2035[2]. Likewise, materials are extracted from the earth, converted to useful products via several energy-consuming processes, distributed, and then, after consumption, lastly discharged to the environment creating a steadily increasing waste stream. Material extraction, production, and use-related release of waste and emission have surpassed the crucial ecological limits[3]. On the other hand, the production of freshwater, extraction, and production of material, and their associated waste treatment consume a considerable amount of energy input, causing a higher risk of environmental change. Overcoming the global scarcity of fresh water, energy, and material resources challenge together with the growing need to develop energy-efficient and environmentally benign processes underscores the utmost necessity to develop advanced and sustainable separation technologies of all sorts.

Among the many potential separation techniques, membrane-based separation is reckoned as the most sustainable technique utilized in diversified water and wastewater treatment[4–6], gas separation[7–11], and material recovery applications[12–14]. A membrane is a semipermeable barrier which, in essence, acts as a perm-selective interface that provides a differential transport resistance to chemical species or components (referred to as permeants), which is the key for membrane-based separations. Unlike conventional separation techniques, membranes separation is considered as cost-effective, energy-efficient, and environmentally benign separation technique[10,15–17] since it avoids the energy consuming phase change process of conventional separations[10] and operates isothermally at ambient conditions[18]. Furthermore, membrane-based separation has several advantages such as simple process, relative ease of operation and control, compact equipment, low energy consumption, and ease of scaling up compared to conventional processes[10].

An ideal separation membrane is characterized by high flux and high selectivity or separation capability. To combine these two desired properties, for several applications, membranes are prepared in the form of thin-film composite (TFC) membrane, which consists of three distinct layers [Figure 1]. TFC membranes structure entails: i) an ultrathin (ca. tens to few hundreds of nanometers scale thick) defect-free top selective layer which mainly dictates the performance of the membrane ii) a highly permeable ultra or micro-porous support layerwhich provides a sufficiently smooth surface to create a defect-free thin top layer (composed of polyacrylonitrile, polysulfone etc), and iii) nonwoven polymeric support made from polyester or polypropylene that merely provides the desired mechanical stability of the composite structure[19]. The ultra-porous sub layer is generally prepared on top of the nonwoven fabric via a phase inversion technique. Unlike integral asymmetric membranes where the selective layer/skin layer and the support layer are composed of a single material, TFC structure provides the opportunity to independently tailor the properties of selective layer and the ultra-porous substructure to obtain a composite with desirable functionalities/features. Surface modification of a microporous membrane allows preparation of a functional membrane with some desired properties for application in nanofiltration (NF), reverse osmosis (RO), solvent resistant NF, ion selective separation[20], micro pollutant removal, gas separation, drug delivery, and as a sacrificial layer.

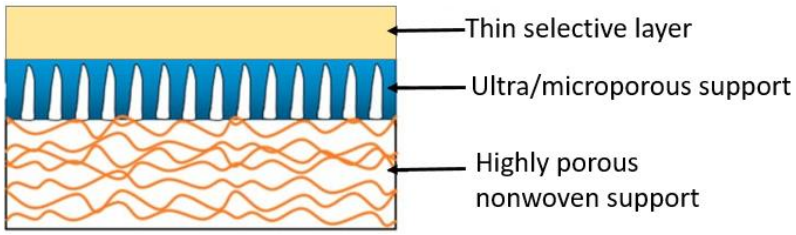

Figure 1. Thin film composite (TFC) membrane

Over the past decades, numerous techniques such as phase inversion[21,22], surface crosslinking, interfacial polymerization[23–25], UV-initiated grafting[26,27], plasma grafting[28], and sol-gel process[29] have been widely used to modify surface of a microporous membranes for designated separation processes.[19] However, most of these methods are costly, laborious and rely on environmentally unfriendly solvents and/or reactions which can partly degrade the support membrane.[30] In this study, a TFC membrane containing a polyelectrolyte multilayer was produced by postmodification

of an asymmetric microporous (PAN) support membrane with polyelectrolytes (PAH and PAA) via layer-by-layer assembly technique. The membrane's hydrophilicity, morphology, chemical structure and surface charge properties of the multilayer membranes was determined. Moreover, the effect of different surface coating parameters such as number of layer and pH of the deposition solution and hydrolysis condition of PAN support on the both water flux and gas (olefin/paraffin) separation performance was thoroughly investigated

1.1 Objectives

The research is aimed to evaluate the utility of polyelectrolyte surface modification of an asymmetric microporous membrane for tailoring its nanofiltration and gas separation performances. Thus, the main objectives of the thesis work were:

1. To investigate the fundamentals of polyelectrolyte multilayer buildup process by characterizing the morphology, surface charge and hydrophilicity of the membranes.
2. To investigate and establish relationships between polyelectrolyte multilayer membrane(PEMM) structure characteristics and membrane performance in terms of water permeance
3. To investigate and establish relationships between PEMM characteristics and gas separation performance in terms of olefin/paraffin separation efficiency
4. To investigate and establish relationships PAN membrane degree of hydrolysis and PEM buildup process

2. Literature review

2.1 Polyelectrolyte multilayer membrane

Polymers are reckoned as a promising membrane material due to their low cost and easy processability compared to inorganic ones. Additionally, the self-assembly of charged polymers is evolving rapidly as a fascinating approach of modifying the surface of membranes by depositing an ultrathin separation layer on a thick, highly permeable, and mechanically robust substrate to provide it with certain desired properties for a designated application. Polyelectrolytes (PEs) are polymers bearing charged or chargeable groups in their repeating unit. These groups can dissociate in polar solvents like water, conveying either positive (polycationic PE), negative (polyanionic PE), or both (zwitterionic PE) charges on the polymer repeating unit while liberating the counter ions into the solution[31]. Furthermore, PEs that are decorated with a high degree of charge

throughout their monomer units, thus fully dissociating at any pH range refer to strong PEs while, in contrast, weak PE contains partially charged repeating units and their dissociation is pH-dependent. Commonly used strong PEs are poly diallyldimethylammonium chloride (PDADMAC) and polystyrene sulfonate (PSS). Whereas poly (allylamine hydrochloride) (PAH), polyethyleneimine (PEI), and polyacrylic acid (PAA) are the regularly used weak PEs.

PEs have curved out a reputation in the preparation of polyelectrolyte multilayer (PEM) membrane via layer-by-layer (LBL) self-assembly of oppositely charged PEs, initially pioneered by Decher and Hong[32] in 1990's. The LBL build of PEM can be performed using several coating techniques, such as dip coating, spin coating and spray coating. In the most common dip coating LBL assembly technique, a charged substrate is alternatively exposed or immersed to oppositely charged PE solutions, followed by an intermediate rinsing with DI to remove excess and weakly adsorbed PEs[33] [Figure 2], assuming negatively charged substrate]. The sequential process is repeated until the desired number of multilayer structure is attained. As explained above, PEs gain charge and entropy by releasing counterions into its surrounding when it dissolves in a suitable solvent[31,34] and subsequently adsorbs onto oppositely charged surfaces due to electrostatic attraction. In principle, the deposition of the first layer neutralizes the opposite charges of the support surface through charge compensation[35,36]. However, only surface charge reversal happens to the bulk material due to charge overcompensation which creates excess surface charge density depending on the terminal PE layer, leaves the surface primed for the deposition of the next PE layer[37,38]. The electrostatic charge neutralization and charge overcompensation drives the polyelectrolyte multilayer buildup process with controlled thickness.

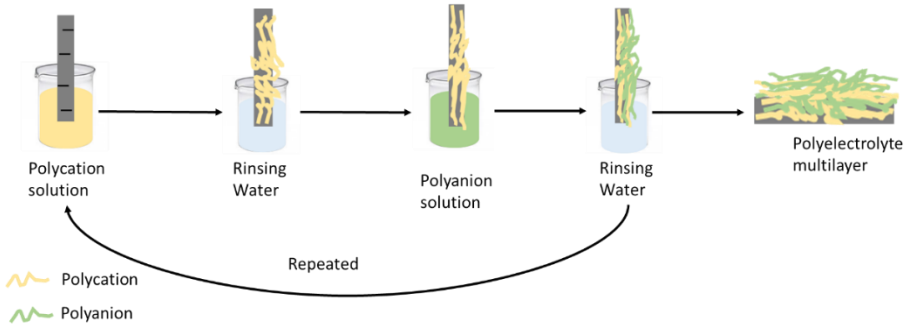

Figure 2. LBL assembly of PEs (dip coating)

Ever since its first report, LBL self-assembly has really established itself as a simple, facile, reproducible, versatile, and efficient approach of fabricating nanostructured thin films with tunable thickness, compositions, structures and properties at the nanometer scale for use in a wide variety of fields such as biomedicine[39], sensor[40], semiconductor, fuel cell[41], membrane separation[31,42], and the preparation of antimicrobial coatings[43].

Compared to conventional membrane modification methods, LBL assembly of PEs allows the deposition of defect free layers, universal and convenient surface chemistry tailoring of various membrane structures[31], and precise control over the thin film thickness down to nanoscale[44]. Furthermore, LBL process utilizes wide range of commercially available versatile PE pairs[45] which are usually low cost and environmentally benign as they are water soluble, needs lower amount of liquid to coat large surface area, and is performed at ambient temperature and pressure except for dynamic assembly[46,47]. PEs can be differentiated in terms of their molecular weight, functional group, charge density etc. Since LBL films are free of any defect, the thickness, and thus the separation performance of PEMM can be finely tailored by tuning numerous conditions such as, number of layers, concentration and of PE, coating method, pH and ionic strength of the coating solution. Therefore, LBL assembly of PEs could be a virtuous technology for fabricating novel functional membranes, as a membrane with high flux, high separation efficiency and good stability is indispensable for practical application. Recently, many researchers have utilized the advantage of numerous available tunable parameters to tailor the surface properties of PEMMs to suit for various scope of applications such as NF[48,49], RO[50,51], gas separation, pervaporation[52,53], SRNF[54], organic micropollutant removal[30], and ion-selective separation[55].

Among the many parameters, rational selection of PE plays a significant role in PEM build up process. This is because properties of the PEM such as thickness, porosity, hydrophilicity, roughness, porosity, hydrophilicity, swellability, and mechanical stability are strongly influenced by the polyelectrolytes (e.g. molecular weight and chain rigidity). Individual PE with high charge density forms strong polycation-polyanion pair which is important to form a relatively thin and more stable PEM structure[56].

Besides the charge density, molecular weight of PEs in the coating solution greatly influences the PEM growth, especially when depositing the first layer. PEs with molecular weight less than the molecular weight cut off value of the support membrane can fill up the porous of the support, thus reducing the

pore size and porosity of the final membrane structure. Such kind of dense PEMM are preferable for pervaporation process as it requires a nonporous membrane. On the contrary, PEs with a relatively higher molecular weight than the molecular weight cut-off of the support membrane can be used to create a porous thin film structure with certain surface charge, which is usually preferable for NF. Similarly, chain length of PE polymer has a significant effect on the performance of PEMM. Wang et al.[57] reported that NF multilayer membrane prepared using static LBL assembly of PEI (branched high Mw) and sPEEK polyelectrolytes on PAN support demonstrated a maximum salt retention of 61% at 3.5 bilayers, while PEMM prepared from low Mw PEI showed no salt rejection at the same number of bilayers. This is mainly ascribed to the better bridging capability of branched PEI polyelectrolytes than linear PEI. On the contrary, linear low Mw PEI form loos structure hence large number of bilayer is required to induce salt rejection.

Next to the type of PE, it is noteworthy considering the effect of various coating parameters on the structure, morphology and separation performance of PEMMs. During LBL assembly, eventual properties of PEM can be precisely controlled by tailoring the ionic strength of the coating PE solution[58–68]. The magnitude of entropy gain of the release of counter ions and charge compensation mechanism are strongly influenced by the ionic strength of the deposition solution. Besides, ionic strength has an additional plus as it affects the ionization behavior of both strong and week polyelectrolytes. To better investigate this, Several researchers have utilized different concentration and type of salts as background electrolyte solution to modify the ionic strength of the polymer solution and reported that charge overcompensation happens due to intrinsic and extrinsic ion balance [Figure *3*] depending on the ionic strength of the PE solution[42,66]. This is because salt screens both the segment–segment repulsion within PEs and the segment–surface attraction between polyelectrolytes and the substrate surface[42].

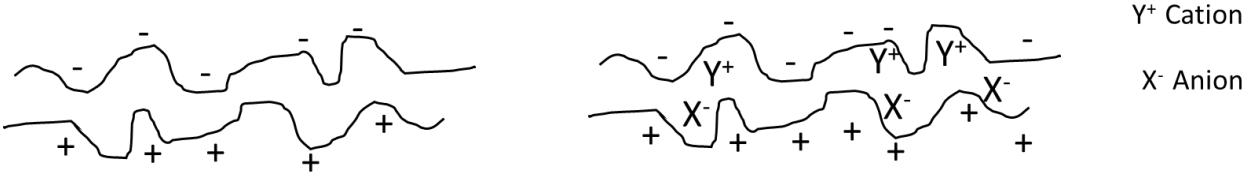

Figure 3. Intrinsic (a) and Extrinsic (b) charge compensation mechanism

In PE solutions with low ionic strength, the segmental attraction between the PEs is strong and charges of the adsorbed polyelectrolytes are mainly balanced by opposite charges from the

adsorbing PE layer, intrinsic charge compensation mechanism[59,66]. During intrinsic charge compensation, thin and dense multilayer layer having a relatively low mobility of the polymer chains is formed. On the contrary, in PE solution with high ionic strength, the entropic gain of counterions upon release is minimum and fewer counterions are released, and thus more counterions remain bound to the polyelectrolyte[69]. As a result, the electrostatic attraction between PE layers is inhibited due to the increase in charge screening of the polymer chains and PE charges are balanced by counter ions in the solution, extrinsic charge compensation[59,66]. Weak electrostatic attraction results in the deposition of greater amount of PEs in coiled and loopy conformation and low surface area per chain, leading to the formation of thick multilayers with more open structure and relatively high mobility of polymer chains[60,66,70–72].

Researchers have prepared application oriented polyelectrolyte multilayer membranes by systematically tailoring the structure and properties of the multilayer film by just modifying the ionic strength of the coating solution. J. de Grooth et al.[60] modified tight ultrafiltration membranes (Hollow Fibre Silica, HFS) with PDADMAC /PSS multilayer using NaCl (0.005, 0.05 and 0.5 M) as background electrolyte solution and observed that, at low ionic strength (0.005 and 0.05M NaCl), the charge compensation happened between oppositely charged polymer chains. The authors reported a transition from intrinsic to extrinsic charge compensation upon increasing ionic strength of the deposition solution from 0.005 and 0.05M to 0.5 M. Such transition is usually accompanied by nonlinear layer growth due to the adsorption of large a amount of PEs leading to the formation of thick and more open multilayer structure. In another study, Remmen et al.[73] studied the influence of ionic strength of the coating solution on scandium (Sc^{3+}) recovery capacity of a 3 bilayer (PDDA/PSS)3 multilayers deposited on a PES membrane by dynamic LbL assembly. They showed that PEMM assembled at high ionic strength (1 M NaCl) demonstrated the highest Sc^{3+} rejection capacity (64%) compared to the thin films assembled at low ionic strength (0.05 M NaCl) which had only 33.7 % Sc^{3+} retention capacity. In addition, the LBL assembled membrane demonstrated good solvent stability and produced water flux of 27 $L/m^2 \cdot h$. at a pressure of 5 bar, highlighting the suitability of LBL assembled membranes for nanofiltration application as the PEMM provides higher flux and selectivity at a relatively lower pressure.

Additionally, LBL assembled PEMM have been considered as ideal nanofiltration membranes for rejecting of multivalent ions, attributed to their size exclusion and charge or Donnan exclusion based ion selectivity capability. Stanton et al.[74] investigated the effect of salt concentration with 4.5 bilayers ([PSS/PAH]4PSS) films coated over porous alumina support. They reported maximum Na_2SO_4 salt rejection up to 95% was obtained by increasing supporting electrolyte concentration (05 – 2.5M $MnCl_2$). This is due to higher surface charge attained upon the deposition of the capping PSS layer. The higher net surface charge was obtained because the terminal PSS layer was less intermingled with underlying layers. However, the water flux decreased with increase in salt concentration, presumably due to increased osmotic pressure.

Interestingly, PEMM membranes prepared using high ionic strength has demonstrated an outstanding separation performance and excellent solvent stability in solvent-resistant nanofiltration (SRNF) application. Li et al.[72] investigated the effect of dipping solution salt concentration on the SRNF performance of PAN based composite multilayered PEC membranes using LBL assembly of SPEEK/PDDA. The composite membrane exhibited an isopropyl alcohol (IPA) permeance increase from 0.06 to 0.98 L/ (m^2 h bar) while maintaining high Rose Bengal (1017 Da) retention with increasing NaCl concentration of the deposition solution from 0 M to 0.5 M. This is mainly ascribed to the looser membrane structure formed as a result of the increase in electrostatic repulsion between the PE chains at high salt concentration.

Besides the ionic strength, it is noteworthy investigating the effect pH of the polyelectrolyte solution on structural and separation characteristics of PEMM, especially when working with week polyelectrolytes. Weak polyelectrolytes are polymers whose charge density is widely tunable from near zero to a fully charged state through simple pH adjustments of their solutions[42]. This affects the solution behavior of the polymer chains and in turn influences their conformation upon adsorption onto the oppositely charged surface. The charge compensation mechanism between two PEs as a function of their degree of ionization in a solution is depicted in Figure 4.

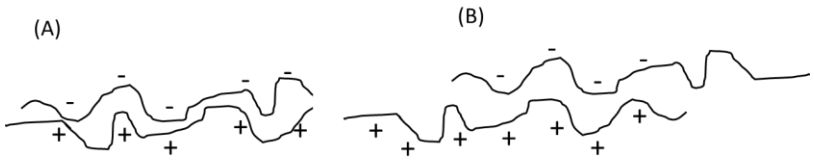

Figure 4. Charge compensation between (a) two fully charged PEs and (b) one fully ionized and another partially charged PEs

Numerous researchers have used the pH of the coating solution as a tunable parameter to systematically control the layer thickness and the molecular structure of the multilayers, which in turn dictates the morphology, structure and overall separation behavior of the membrane. Furthermore, the charge density and structure of weak PEMMs can be modified by varying the environmental pH after build-up[75].

Shazia Ilyas et al.[54] studied the solvent resistant nanofiltration (SRNF) performance of hydrolyzed PAN membrane modified with weak polyelectrolytes multilayers prepared from PAA and PAH solutions of pH (PAH/PAA: 7.5/7.5, 7.5/3.5 and 3.5/3.5) and polymer concentration of 0.1 g l^{-1} in a 50 mM $NaNO_3$. Films assembled at pH of PAH/PAA: 7.5/7.5 were 8 times thinner than the films formed at other pH combinations. Sanyal et al.[76] also modified NF 90 commercial membrane with 5-bilayers of PAH/PAA films prepared from a solution at a pH of (PAA/PAA: 8.5/3.5 and 6.5/6.5) and reported that the lowest film thickness was obtained at pH combination of 6.5/6.65. This is because PAH with pKa 8–9 and PAA with pKa of 4.5 are nearly fully charged at this pH range and thus forms a stretched conformations due to high electrostatic repulsions between charged segments of the PEs[54,77,78]. Furthermore, small amount of PE is required to compensate for all charges existing in the previously deposited layer, intrinsic charge compensation mechanism. On the other hand, thick and loopy film structure was demonstrated at a deposition solution pH combinations of (PAH/PAA: 7.5/3.5[54] and 8.5/3.5[76]) owing to the partially charged configuration. As a result, the membranes produced at pH conditions of PAH/PAA: 7.5/7.5 had the highest SRNF separation performance along with good solvent stability in solvents such as isopropyl alcohol (IPA), acetonitrile (ACN), tetrahydrofuran (THF) and in the challenging polar aprotic solvent, N,N-dimethylformamide (DMF) due to the lower extrinsic charge compensation. The pure IPA permeance values were: 7 L m^{-2} h^{-1} bar^{-1} for [7.5/7.5] membranes, 4 L m^{-2} h^{-1} bar^{-1} for [7.5/3.5] membranes, and 5 L m^{-2} h^{-1} bar^{-1} for [3.5/3.5] membranes. These permeance results suggest that the film was not only thin but also denser than the others[54].

Generally, as reported by Rubner et al.[77] [Figure 14, appendix], thin and dense film structure is formed at a pH combination where both the Polyelectrolytes are equally or fully charged. At this pH combination, there exists a strong electrostatic repulsion between the fully charged polymer segments and as a result the segments form a stretched/extended conformation. On the other hand, thick and loopy structure is formed when one of the PE solution is in a fully charged situation while the second one is only partially charged, thus large amount of the second electrolyte is needed to compensate the charges from the adsorbed layer.

Furthermore, it is important to mention that researchers have introduced new methods of preparing LbL assembled PEMMs with the intention of speeding up and scaling up the coating process. Dynamic coating of PE, which is based on alternating filtration of PE solution under pressure is considered as the best option to uniformly coat a large membrane area at a relatively short period of time compared to the common static one[46,79–81]. Ji et al.[81] modified PAN ultrafiltration membrane using alternative filtering PEI and PAA polyions in a dead-end filtration cell under a pressure of 0.1MPa. They reported that the regularity of the membrane surface was enhanced and the resulting membrane can maintain a stable performance up to 52 h for dehydration of a 95% ethanol aqueous solution. In another study, Su et al.[80] used cross-flow dynamic assembly to modify the surface of polysulfone (PS) membrane with a single layer of PDADMAC polyelectrolyte. Surface zeta potential measurement revealed that the membrane prepared by the static method demonstrated a negative zeta potential due to the stronger negative charge of the PS membrane, shielding some of the positively charged amino groups of the PDADMAC. However, the dynamically assembled film produced a positive surface charge of +55 mV, signifying the remarkable impact of the type of coating procedure used.

Finally, LbL build of PEMMs involves the use of wider range of almost any kind of any shape charged substrates such as poly(ethersulfone), sulfonated poly(ethersulfone), polysulfone, plasma-treated poly(acrylonitrile), and porous alumina supports, as a result, the separation performance of PEMMs is highly dependent on the surface properties of substrate. In addition to the commonly needed thermal, mechanical, chemical stability combined high permeability, it is preferable to use charged and low surface roughness support membrane for constructing polyelectrolyte

multilayers. The effect of support surface charge is usually limited to the adhesion of the first. To obtain a support with such surface characteristic, several process such as alkaline hydrolysis of [82,83] and allylamine plasma polymerization[84] have been applied to post-modify surface of PAN and Poly(tetrafluoroethylene) PTFE support membranes. Alkaline hydrolyzed microporous Polyacrylonitrile membrane was employed as a porous substrate in this thesis work.

In this study, a new roll-to-roll (R2R) based layer by layer assembly was employed to coat large areas of flat sheet microporous PAN membrane with very thin polyelectrolyte films. Considering the flexibility to modify the properties of weak polyelectrolytes by changing some external parameters such as pH and ionic strength of the coating solution and the environment during deposition and after the build-up, respectively, weak PEs PAA and PAH were chosen in this work. It should be noted that this combination has been used to modify PAN membrane. However, the effect of R2R assembly on the structural properties, olefin/paraffin separation has not, to the best of this work, been described.

3. Experimental part

3.1 Material and chemicals

An in-house prepared polyacrylonitrile (PAN) microfiltration membrane was used as a porous support membrane. Weak polyelectrolytes poly (allylamine hydrochloride) (PAH, Mw = 50,000 g mol^{-1}) and Polyacrylic acid (PAA, Mv=450,000 g mol^{-1}) were purchased from Sigma-Aldrich, Germany. The chemical structures of these polyelectrolytes is shown in Figure 5. 5mM NaCl salt was used as background electrolyte to prepare the PE solutions. NaOH and HCl were used to adjust the pH of PE solutions. All chemicals were also obtained from Sigma-Aldrich, Germany were used as received without further purification. Deionized water (conductivity of 0.055 μΩ cm) was used for membrane rinsing and preparation of PE solutions.

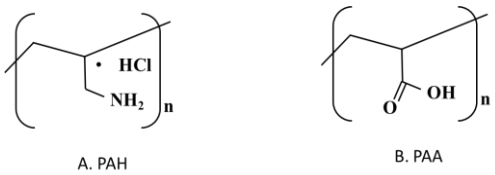

Figure 5. Chemical structures of PEs used in this work.

3.2 PAN membrane post modification

The polyacrylonitrile (PAN) microfiltration membrane was firstly chemically postmodified using alkaline hydrolysis method to improve its surface charge[85] following the previously reported procedures[86]. Briefly, PAN membrane was immersed in 2 M NaOH solution for various periods of hydrolysis time (1, 1.5, 2, 2.5, and 3 hr.) in order to gain the initial knowledge and experience to choose best hydrolysis condition for its post functionalization. Subsequently, the membranes were thoroughly rinsed with excess amount of distilled water several times to remove any residual NaOH solution. The hydrolyzed membranes were dried at room temperature for 30 minutes before coating.

3.3 PEMM via Layer by Layer Assembly

The PEMM buildup was performed in an in-house-built laboratory scale roll-to-roll (R2R) dip coating machine[Figure 6], at room temperature. The R2R dip coating machine consists of deposition solution holder and two guiding rolls, one stationary roll to place the membrane in a frame so that only its top surface is exposed to the polyelectrolyte coating solutions. Typically, a flat sheet membranes with a length of up to 100 cm and width of up to 10 cm can be coated with this device. During the coating process, the coating solution was applied just to the selective side of the support by creating a meniscus between the belt shaped rolling HPAN membrane and the PE coating solution. The speed was adjusted to the desired constant path velocity automatically by the controller.

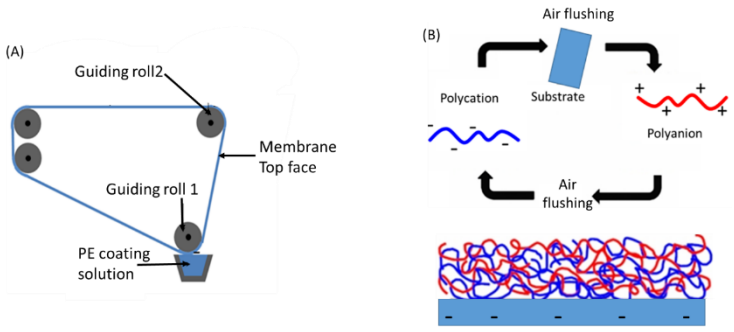

Figure 6. Schematic representation - (A) Roll-to-Roll (R2R) dip coating machine developed at Institute of Membrane research, Helmholtz Zentrum Hereon and (B) cycle of multilayer buildup process, assuming negatively charged substrate

Due to the pH dependent degree of ionization of weak polyelectrolytes and the subsequent coating conditions, different solutions of PAH and PAA were investigated in order to gain the initial

knowledge and experience to choose three PE solution pH combinations to prepare the PEMM. Specifically, PAH and PAA solutions containing 0.15wt. % PE were first prepared in 0.005 μΩ micropore water and 5mM NaCl as supporting electrolyte. The pH of the PE solutions was adjusted (2.5 – 8.5) using either 1M HCl or 1M NaOH solution by dropwise technique. The PE solutions were stirred for 15 minutes at room temperature and no precipitation or clouding was detected in the PE solutions.

Briefly, during the R2R assembly, the top surface of the HPAN was first exposed to the pH adjusted polycation (PAH) solution and was allowed to roll a full cycle at a controlled speed to coat the whole membrane area. Next, the PAH modified membrane was exposed to the negatively charged (PAA) solution in a similar manner. This produced one PAH/PAA "bilayer" (BL) and the procedure was repeated till the desired PAH/PAA coatings of target thickness were obtained on the membrane. No intermediate washing was employed since it has no or near negligible effect on overall performance of PEMMs[87,88]. Furthermore, it minimizes chemical consumption (NaCl, HCl and NaOH) and related waste release as high amount of washing solution is needed to completely rinse the whole membrane. Finally, the membranes were dried using a multi-step process. First, they were dried by air flushing for 5 min and further dried in ambient air for 1 hour followed by vacuum oven drying at 40 for an additional overnight.

To study the effect of pH of the deposition solution on the buildup process of PAH/PAA multilayer, different pH combination (1. equal pH of both polyelectrolytes (2.5/2.5, 4.5/4.5, 6.5/6.5, and 8.5/8.5), 2. Constant pH of PAH polyelectrolyte solution coupled with varying pH of PAA solution, and 3. Constant pH of PAA polyelectrolyte solution coupled with varying pH of PAH solution) were used. Based on the preliminary experimental result, three pH combinations (PAH/PAA: 2.5/4.5, 6.5/6.5, and 2.5/8.5) were selected to study the effect of coating solution pH on the structure and overall separation characteristics of the as prepared PEMMS. In this thesis, the multilayer membranes are designated as (PAHy/PAAz) , where y and z are pH of PAH solution, pH of PAA solution, respectively. For instance, (PAH2.5/PAA6.5) represents a PEMM assembled from PAH and PAA solutions of pH 2.5 and 6.5, respectively.

3.4 Characterization of the membranes

3.4.1 Scanning Electron Microscopy (SEM)

The surface and cross-sectional morphologies of the all membranes including pristine, hydrolyzed, and PEMM were characterized with the help of scanning electron microscope (SEM) instrument after oven drying at 40 for 48 hours. Secondary electron (SE) images of SEM were taken at voltage of 3 kV. For the cross-sectional analysis, the samples were fractured in cryogenic liquid nitrogen. Before examining the samples were prepared by coating a thin layer of 1.5 nm platinum using Safetamtic CCU-010, Switzerland, to promote conductivity.

3.4.2 Fourier Transform Infrared Spectroscopy (FTIR)

The chemical structure of the pristine and hydrolyzed PAN membranes was investigated by Attenuated Total Reflectance Fourier transforms infrared spectroscopy (ATR-FTIR-diamond crystal) mode equipped with an ATR unit to see the chemical changes happening due to alkaline hydrolysis. FTIR spectra of the membranes were collected in the range of 4000–400 cm^{-1} with a nominal resolution of 2 cm^{-1} and average scan of 32 at room temperature.

3.4.3 Streaming Potential Measurements

Surface zeta potential (ZP) of the membranes was determined using an Electrokinetic analyzer (Anton Paar, SurPASS 3, Germany) with 0.168 mM NaCl solution in DI water as background electrolyte and room temperature condition. The membrane samples were analyzed for 4 measurement cycles in the pH range of 3 to 9 to eliminate experimental error. The pH values were adjusted using 50 mM HCl and 50 mM NaOH solutions in a range of 4 – 10. The adjustable streaming channel gap height was fixed in a range between 95-105 µm.

The surface zeta potential (ζ) was determined from the streaming potential (U_{str}) using the Helmholtz-Smoluchowski equation 1:

$$\zeta = \frac{d\mathrm{U_{str}}}{d\Delta P}\frac{\eta}{\varepsilon\varepsilon_0}\frac{l}{A}\frac{1}{Re} \qquad \text{Eq. 1}$$

where ΔP is the pressure difference across the streaming channel (Pa), η is the dynamic viscosity of the electrolyte solution (Pa·s), ε is the permittivity of the electrolyte, ε_0 is the vacuum permittivity ($F \cdot m^{-1}$), *l* is the length of the streaming channel, A is the cross section of the streaming channel (m^2) and Re is the electrical resistance inside the streaming channel.

3.4.4. Contact Angle measurement

The water contact angle of all membranes was measured using sessile drop method on a Krüss Drop Shape Analysis System DSA 100. As mentioned above, membranes were dried before the measurement to make sure it was free of humidity. Milli-Q water (2 µl) was dropped at a speed of 2.67 µL/s at three different location of the same membrane surface utilizing a syringe to check the formation of uniform surface coating and the mean value was considered as the result.

3.4.5 Gas Permeation testing

PAH/PAA PEMMs were characterized in terms of their gas permeance (methane, ethane, ethylene, propane, and propylene) at 23 °C. Single gas permeation experiments were carried out with pure gases using pressure increase measurement facility built in-house, Helmholtz Zentrum Hereon, Germany[89]. The basic principle is based on constant volume-variable pressure method i.e. measuring the pressure increase rate on the defined volume permeate side of the thermostated membrane cell when certain feed pressure is applied to the membrane[90–92]. In order to clean the permeation system, both sides of the membrane cell were evacuated before the start of the measurement using vacuum pumps. During the experiment, the feed pressure was maintained at 1000 mbar for all gases. Next, valves were opened to allow the feed gas to flow into the membrane cell which has an effective membrane area of 3.21 cm^2. Thus, gases permeate through the membrane and are collected in the initially evacuated permeate vessel. The pressure increase in the permeate side at constant feed pressure was automatically recorded as a function of time by the machine. Single gas permeance data was obtained by automatic acquisition of permeation data points at each pressure increase step of the permeate side between 1-10 mbar at 23.5 ºC.

The single gas permeance P (m^3 (STP) m^{-2} h^{-1} bar) and ideal selectivity ($\alpha_{A/B}$) of the membrane for pure gases A and B were determined using the equation the Equation (2) and (3):

$$P = \frac{V_p 22.4}{RTA\Delta t} \ln\left(\frac{p_f - p_o}{p_f - p_{p(t)}}\right) \qquad \text{Eq. 2}$$

$$\alpha_{A/B} = \frac{PA}{PB} = \frac{DASA}{DBSB} \qquad \text{Eq. 3}$$

where V_P is the constant permeate volume [cm^3(STP)], l is the film thickness (cm), A is the effective area of membrane (cm^2), R is the gas constant (8.314 J mol^{-1} K^{-1}), P_f is pressures at the feed, P_o is permeate pressure at the beginning of the measurement , $P_{p(t)}$ is permeate side at the end

of the measurement, and Δt is the time for permeate pressure increase from p_o to $P_{p(t))}$ (s). The factor of 22.4 is used to convert from molar to volumetric units.

3.4.6 Pure water permeance measurement

The hydrolyzed HPAN support and PEMMs were characterized in terms of their pure water permeance (L m^{-2} h^{-1} bar^{-1}) using a home-made dead-end filtration system, with 1.77 cm^2 active membrane area and a trans-membrane pressure of 4 bar at room temperature. The applied transmembrane pressure was controlled with a pressure regulator. The experiment was allowed to run until the weight of the permeate volume reaches 1000 g, while gravimetrically measuring the volume change ΔV at every 3 minute. The pure water flux (J_0) (L m^{-2} h^{-1}) was determined by measuring this permeate mass, calculating permeate volume using equation (4):

$$J_0 = \frac{\Delta V}{A \Delta t} \qquad \text{Eq. 4}$$

The water permeance (Jw), (L m^{-2} h^{-1} bar^{-1}) was determined by normalizing the pure water flux by the transmembrane pressure, equation (5).

$$J_w = \frac{\Delta V}{A \Delta t \, \Delta P} \qquad \text{Eq. 5}$$

4. Result and Discussion

In this study, PEMMs were prepared by LbL assembly of polyelectrolytes on top of asymmetric microporous PAN support while varying the pH of the coating solutions to tune the charge density and structure of PEs, and thus further control the structure and separation performance of the resulting TFC membranes. The microporous PAN membrane was selected as a base membrane due to its high degree of solvent stability, mechanical stability, and relatively cheaper price than other conventional polymers like poly (sulfone) and poly(ether sulfone)[93,94]. In addition, LBL assembly of PEMM requires a substrate with certain surface charge opposite to the PE charge that provides the desired electrostatic interaction with the polyelectrolyte for depositing the first monolayer in order to get good adhesion of the first layer[46]. Hence, the suitability of PAN support [Figure 7(a)] for constructing the multilayer membrane was studied prior to its modification with PE layer.

Initially, assuming the PAN membrane contains some inherent negative surface charge, the PAN membrane was directly coated with PAH polyelectrolyte. The PAN/PAH demonstrated poor surface coverage indicating meager deposition of PAH PE [Figure 7 (b)]. The poor coating could be due to the penetration of the polyelectrolytes into the pores of the support membrane. Therefore, the PAN membrane was coated with branched polyethyleneimine (PEI) polyelectrolyte (Mw= 25, 000 g mol^{-1}) as an intermediate layer to avoid pore filling problem. Besides, the deposition of branched of PEI as a first layer can assist to successfully seal the pores of the membrane without penetrating into the pores of the substrate and offers uniform surface for successive deposition[95]. PEI was cross-linked with glutaraldehyde to enhance the membrane stability. On the other hand, the PAN/PEI membrane was highly dense [Figure 7 (c)] most likely due to the penetration of PEI through the pores . Not only the surface but the whole PAN layer was sealed with crosslinked PEI. This was not the goal.

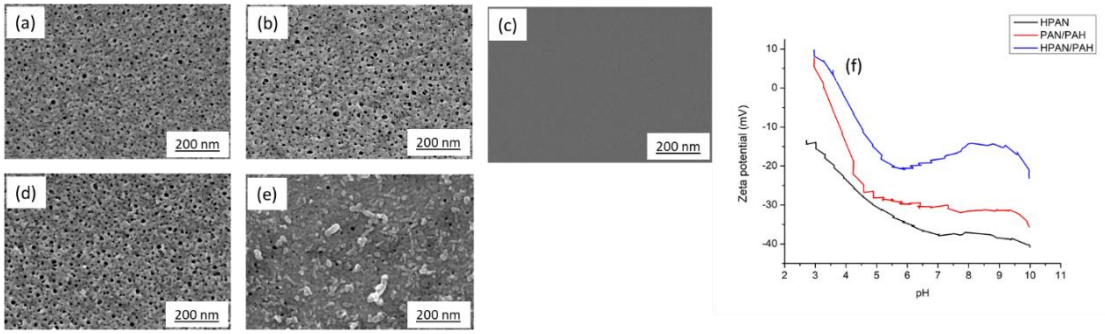

Figure 7. SEM surface image of membranes: (a) Pristine PAN, (b) PAN/PAH (c) PAN/PEI, (d) PAN/PAH dipped in water for 4 days, (e) HPAN/PAH dipped in water for 4 days, (f) Zeta potential of HPAN and the water dipped PAN/PAH and HPAN/PAH membranes. All SEM images are taken at 100kx magnification.

Therefore, it was decided to post-modify the PAN membrane to achieve high negative surface charge before deposition in order to improve the adhesion of the first PAH layer. PAN membrane was chemically modified using alkaline hydrolysis to generate negative charges at the substrate surface to make it able to anchor the first PAH layer. Next, both pristine PAN and hydrolyzed PAN (HPAN) membranes were coated with single PAH layer and dipped in distilled water for 4 days to see the benefit of alkaline hydrolysis in improving the adhesion of the first layer. Strong electrostatic interaction or adhesion enhances stability of the membranes. The membranes were compared in terms of their zeta potential, morphology and gas separation efficiency.

As can be seen from Figure 7 (e), better surface coverage was achieved in the hydrolyzed membrane even after dipping in water for 96 hr. The roughness detected on the surface of

HPAN/PAA [Figure 7 (e)] membrane indicates the presence of function group clusters from the terminal PAH polyelectrolyte. Besides, the HPAN/PAH membrane demonstrated permeance of 45, 50, 47, and 48 GPU for ethane, ethylene, propane and propylene gases, respectively. This is in line with the zeta potential result shown in Figure 7 (e), where the the surface of PAN/PAH was not covered with PAH because the PAH was washed away. But the surface of the HPAN/PAH was covered with PAH. On the contrary, no gas permeance data was recorded in the PAN/PAH membrane since all feed gasses passed through it during the first pressure increase. In addition, the HPAN/PAH had an isoelectric point at pH 3.8 and exhibited higher positive and lower negative surface than the PAN/PAH membrane in the whole pH range [Figure 7 (f)]. Isoelectric point of the PAN/PAH membrane was at and 2.9 and exhibited lower positive surface charge than HPAN/PAH even at pH less than 3.28 [Figure 7 (f)]. The results suggest that surface hydrolysis can improve the adhesion of PAH layer on top of the macroporous PAN membrane.

Therefore, this section is divided into three parts. The first part discusses about the optimization of PAN membrane hydrolysis conditions. The second part deals with the fabrication and characterization of the PEMMs via SEM, zeta potential, and contact angle measurements. In third part the separation performance of the membranes in terms of pure water permeance and gas permeation is discussed.

4.1 PAN membrane hydrolysis

The PAN support membrane was chemically modified with aqueous NaOH solution to introduce negative surface charge by converting the polar nitrile (–CN) groups present in the pristine PAN to carboxylic ($–COO^-$) groups. The surface SEM image of the PAN membranes modified using 2M NaOH alkaline solution and hydrolysis time between 1 and 3 hr. is shown in Figure 8**Error! Reference source not found.** Except the slight decrease in number of pore, no significant change was observed in the surface structure of the membrane until hydrolysis time 1.5hr [Figure 8(b-c)]. At hydrolysis time 2 hr. more pores with a relative narrow size distribution were detected [Figure 8 (d)]. After wards, at hydrolysis time higher than 2 hr. the membrane displayed an irregular pores with a large size distribution [Figure 8(e-f)], ascribed to the conversion of some PAN molecules into poly(acrylic acid) dissolved in water[96]. Although an ideal support layer is required to possess a relatively high surface porosity, this large pore size is accompanied by certain limitations such

as penetration of the top layer material into the pores of the substrate and the problem of achieving defect-free thin film coating[96]. This suggests to find a compromise between the alkaline concentration and hydrolysis time. Hence, suitable hydrolysis time was selected by observing the chemical characteristics of HPAN membranes using FTIR analysis.

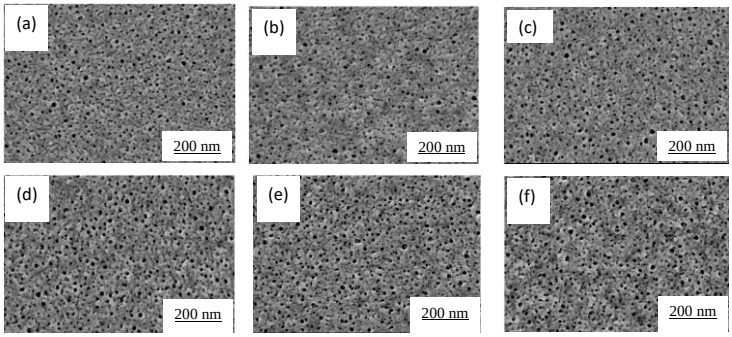

Figure 8. SEM micrographs of top surface of (a) untreated PAN and (b), (c), (d), (e) and (f) are HPAN membranes hydrolyzed under 2M NaOH alkaline solution and hydrolysis time of 1, 1.5, 2, 2.5 and 3 hr., respectively. All images are (100kx) magnification.

ATR-FTIR analysis was used to study the surface chemistry of the HPAN membrane in order to confirm the formation of the desired carboxyl-enriched functional groups that are of a great interest for more demanding subsequent modifications in this study[30]. Figure 9 shows the FT-IR spectra of the pristine PAN and the NaOH treated HPAN membrane under different hydrolysis conditions. For the untreated PAN membrane, the sharp, strong characteristic peaks at 2242 cm^{-1} and 1455 cm^{-1} could be attributed to the C-N stretching vibration of the C≡N group. These peaks were there [Figure 9 (a-f)] signifying the incomplete conversion of C≡N group. After 1 h of alkaline hydrolysis (Figure 9 (b-d), new peaks at 1565 and 1669 cm^{-1}, corresponding to the asymmetric (C=O) stretching band of carboxylate group[97] and –C=N stretching[98], respectively, appeared confirming the formation of (–C=N) before carboxylic (-COOH) group. The intensity of –C=N stretching increases until hydrolysis time of 2 h and thereafter rapidly decreases as amide and carboxyl groups are formed. On the other hand, the intensity of the peak at 1565 cm^{-1} increases sharply for a higher reaction time evidencing the formation of $-COO^-$ ion[99] via hydrolysis of NaOH solution. Furthermore, the characteristic broad –OH stretching peak at around 3300 and the C-H stretching peak 2932 cm^{-1} in the HPAN membrane which are attributed to the stretching vibration of –OH and C-H, respectively, increased with hydrolysis time and provided strong evidence that carboxyl groups formed as a result of hydrolysis reaction. As noted from the FTIR spectrum analysis, the hydrolysis reaction was happened in two steps i.e. the formation of intermediate amide moiety

followed by its subsequent conversion into amide and carboxyl group at higher reaction time. To conclude, the amount of COO- group was increasing with increasing in hydrolysis time.

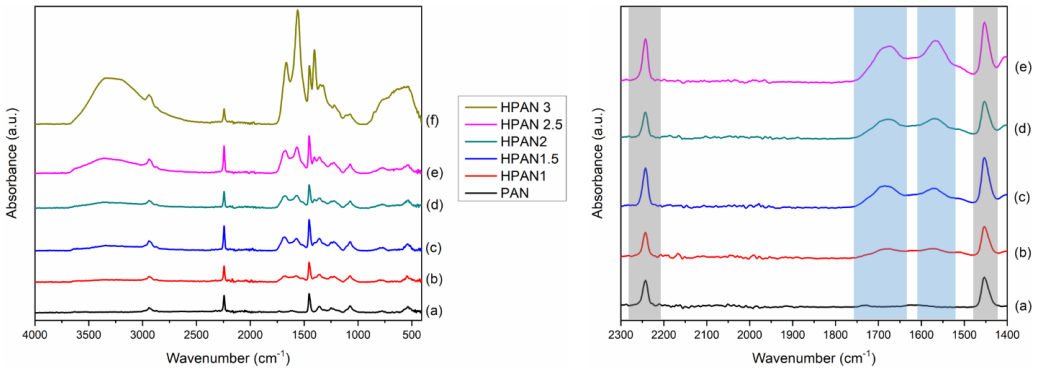

Figure 9. The FTIR spectra of pristine and alkaline hydrolyzed PAN membranes

Lastly, taking together the SEM and FTIR result, it was shown that the alkaline hydrolysis affects both the chemical and morphological characteristics of the membrane. Therefore, the hydrolysis condition selected during this thesis was 2M NaOH and 2h hydrolysis time. Since the morphological behavior of the membrane was not significantly changed at this hydrolysis time. Cross-section and surface SEM image of HPAN membrane is available in Figure 15 in appendix. To further validate the selection, the hydrophilicity of the HPAN membrane was compared with literature. Initially, the pristine PAN membrane exhibited a water contact angle around 67.95^{o} while after hydrolysis with 2M NaOH solution for 2 h, the contact angle decreased to 34.82^{o}, which is in good agreement with Abtahi et al[30]. This can be credited to the hydrophilicity property of the polar carboxyl groups created on the HPAN surface. This improvement of membrane hydrophilicity could potentially boost the water permeation through the membrane.

4.2 PEMM Fabrication

After optimizing the PAN membrane hydrolysis conditions, the negatively charged HPAN membranes were coated with PAH/PAA multilayers via a roll-to-roll (R2R) dip coatingmachine. The formation process and properties of a polyelectrolyte multilayer membrane as a function of each deposited layer is conferred below. The surface properties of membranes were characterized using SEM, Zeta potential, and contact angle measurements.

4.2.1 Single layer deposition

The surface and cross-sectional morphologies of the PE coated membranes were characterized with the help of scanning electron microscope (SEM). Due to time limitation, only the PEMMs prepared from coating solution pH combinations of (2.5/4.5, 2.5/8.5, and 6.5/6.5) were critically characterized to study the multilayer fabrication process. To begin with, Figure 10 show the cross section (top) and top surface (bottom) images, and zeta potential (left) of HPAN membranes modified with a single PAH layer prepared from a polyelectrolyte solutions of pH 2.5 and 6.5 and 5mM NaCl background electrolyte concentration. As can be clearly seen from the cross section images, both membranes exhibit an asymmetric membrane structure which contains a top layer and porous support layer with sponge like structure. This confirms the deposition of PE layers on the surface functionalized PAN support membrane. This asymmetric architecture of membrane helps to obtain high rejection/selectivity using the top skin layer combined with high flux owing to the porous structure in its cross-section.

The characteristic uniformity and homogeneity of top layer appeared to vary with the pH of the coating solution. Poor surface coverage was observed after coating with PAH solution at pH 2.5, unexpected result [Figure 10(b)]. According to its pKa value (8-9), PAH becomes fully ionized at pH 2.5 and thus occupies a more extended conformation due to the electrostatic charge between its charges. Unlike the obtained result, this extended conformation was expected to give good surface coverage. It was not possible to provide a logical reason for this strange result. But there appears to be some polyelectrolyte in the internal part of the support as the brightness observed in [Figure 10(a)] is likely due to a small amount of polyelectrolyte deposition [Figure 15 (b)] for comparison). However, the majority of film deposition occurs at the support surface not in the inside the pores [Figure 10(b)]. On the contrary, better surface coverage was achieved after coating with a single PHA layer at pH solution of 6.5 [Figure 10(d)]. Here again at pH 6.5, PAH exists in a nearly fully ionized situation but in a little less stretched conformation than at pH 2.5[77]. Therefore, it is reasonable to obtain good surface coverage with some defects which are inevitable during the deposition of first PE layer in LBL assembly of PEMMs.

Similarly, zeta potential results also support this findings. The support modified with PAH2.5 layer demonstrated higher negative surface charge at pH higher than its isoelectric point (ca. 4.5) compared to PAH6.5 which had an isoelectric point of ca. 5.3 [Figure 10(e)]. This means the

PAH2.5 coated membrane still assumes the surface properties of the support membrane as can be seen from their closer negative zeta potential value in the pH range (9-5) [Figure 10(e)]. On the contrary, the PAH6.5 coated membrane exhibited lower negative surface charge and achieved fast charge reversal indicating to the good deposition of PAH its corresponding deposition to $-NH_2$ at pH below 5.3. The positive surface charge or charge reversal observed at lower pH in both membranes further confirms the deposition of PAH layer on top of the hydrolyzed membrane. Furthermore, contact angle of the membranes increased from 34.82^o of HPAN to 50.51 ^{o} and 62.17 after coating with PAH2.5 and PAH6.5, respectively. The increase in membrane hydrophilicity indicates the decrease in the amount of polar carboxyl surface charge due to the charge neutralization from the positively charged PAH adsorbing layer. The relatively lower contact angle in PAH2.5 film indicates that the surface characteristics of the membrane is still influenced by the substrate properties.

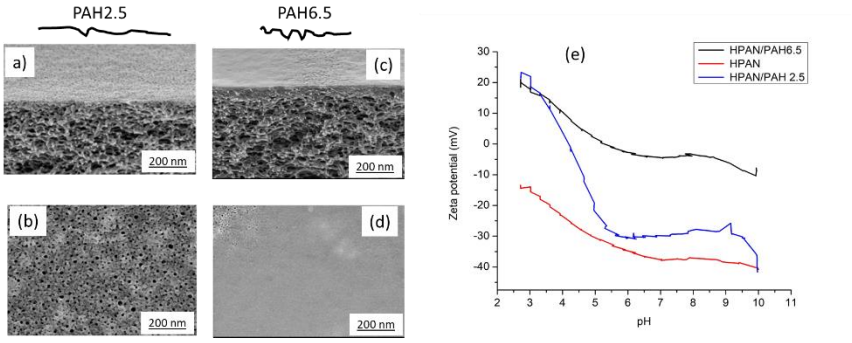

Figure 10. SEM image: cross section (a) and surface (b) of HPAN/PAH2.5, cross section (c) and surface (d) of HPAN/PAH6.5, and Zeta potential (e) of HPAN and the other single layered membranes prepared from 0.15 wt. % PE in 5mM NaCl salt solution

4.2.2 Second layer deposition

Next, the single layered membranes were modified with successive layers of PAA solution to produce a bilayer membrane structure. The HPAN/PAH2.5 membrane was coated with PAA solution of pH 4.5 and 8.5 to produce (PAH2.5/PAA4.5 and PAH2.5/PAA8.5), while HPAN/PAH6.5 was coated with only PAA 6.5 to get PAH6.5/PAA6.5. The SEM and zeta potential of all membranes is depicted in [Figure 11]. In contrast to the single layered membranes shown in Figure 10, there were no apparent pores after the deposition of second PAA layer [Figure 11], indicating the formation of dense and compact multilayer film on top of the hydrolyzed membrane. Thus, this suggests that PE films of at least one bilayer thick are necessary to completely cover the pores of the microporous support.

Another observation from the SEM images of PEMMs is the thickness appears to increase with the increase in number of layers, ascribed to the large amount of PE deposited. Upon comparing the thickness of the three membranes, the PAH6.5/PAA6.5 membrane demonstrated a relatively thinner layer. This is ascribed to the nearly equal (nearly 80–90%) degree of ionization of PAA and PAH polyelectrolytes in this pH combination that leads to high charge crosslinking density between the polymer chains[95]. In contrast, in PAH2.5/PAA4.5, the adsorbed PAH layer exists in a fully ionized state whereas PAA at 4.5 is only partially charged, and thus lower amount of charged segment of the PAA chain was adsorbed or penetrated into the previous PAH layer while its non-charged part extends away from the surface in the forms a tail and coil structure[77]. It should be noted that the PEs attempt to reduce their pKa when they are deposited in an attempt to neutralize the charges existing in the adsorbed layer. Another reason for the higher thickness in this pH combination is higher amount of PAH is adsorbed to compensate the charges the charges from the previously adsorbed layer. Although, thinner layer was expected in PAH2.5/PAA8.5 than in PAH2.5/PAA4.5, no substantial difference was observed.

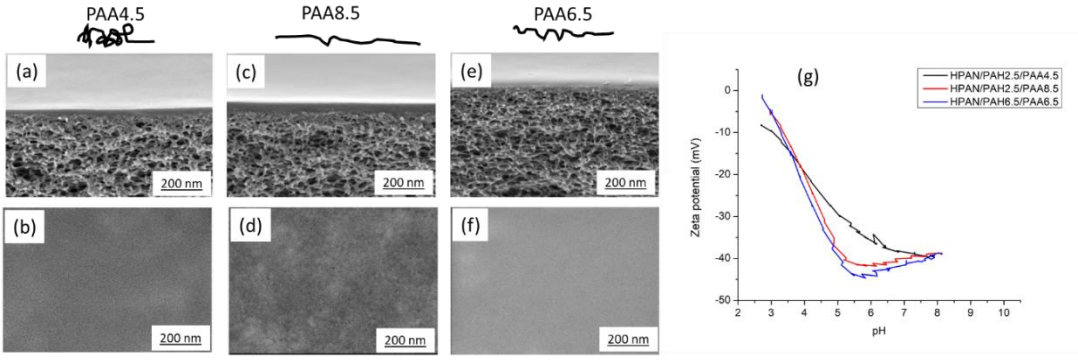

Figure 11. SEM image of PEMMs: cross section (a) and surface (b) of (PAH2.5/PAA4.5)2, cross section (c) and surface (d) of (PAH2.5/PAA8.5)2, cross section (e) and surface (f) of (PAH6.5/PAA6.5)2, and Zeta potential (g) of all membranes prepared from 0.15 wt. % PE in 5mM NaCl salt solution

Moreover, surface the zeta potential of the membranes revealed negative surface charge throughout the whole pH range [Figure 11 (g).]. This indicates that the membrane surface properties are dominated by the terminal PAH layer. Less negative surface charge was observed at low pH indicating poor dissociation of PAA at low pH. In addition, the contact angle of the membranes displayed a decline after coating [Figure 16] in appendix. The PAH2.5/PAA4.5 demonstrated better hydrophilicity, while PAH6.5/PAA6.5 was the least hydrophilic one. This is ascribed to the excess surface charge produced due the high extrinsic charge overcompensation occurring between the fully charged PAH (pH=2.5) and partially charged PAA (pH=4.5) polyelectrolytes. On the

contrary, at pH combinations of both (6.5/6.5) and (2.5/8.5), higher intrinsic charge compensation occurs during the LBL assembly of nearly equally or fully charged PAH and PAA PEs , and consequently lower amount of -NH_2 and –COOH exists on the membrane surface[100].

4.2.3 Third layer deposition

Moreover, the membrane were coated with successive PAH layer with the same solution pH (2.5 and 6,5) to increase the membrane thickness for the purpose of improving its separation performance. In the three layered PEMMs the SEM images revealed an increase in surface roughness as the number of layer increase [Figure 12]. It is an expected trend to observe an increased surface roughness with increasing number of layers, due to the presence of excess surface groups. The nonhomogeneous surface observed in Figure 12 is ascribed to the excess positive surface charge existing in the PAH capping layer which can lead to swelling of the structure. This could also be due to accumulation of small PEs[101]. Some pinholes were observed in Figure 12 (a) HPAN/PAH2.5/PAA4.5/PAH2.5. It is difficult to give physical interpretation for this non-uniform surface coverage. However, this membrane demonstrated higher positive surface charge at a pH below its isoelectric point.

Another observation from the SEM images of PEMMs is the thickness appears to increase with the increase in number of layers, ascribed to the large amount of PE deposited. The contact angle of the membranes again increased to a higher value showing the effect of PAH terminal layer. However, (PAH6.5/PAA6.5) was still the least hydrophilic one.

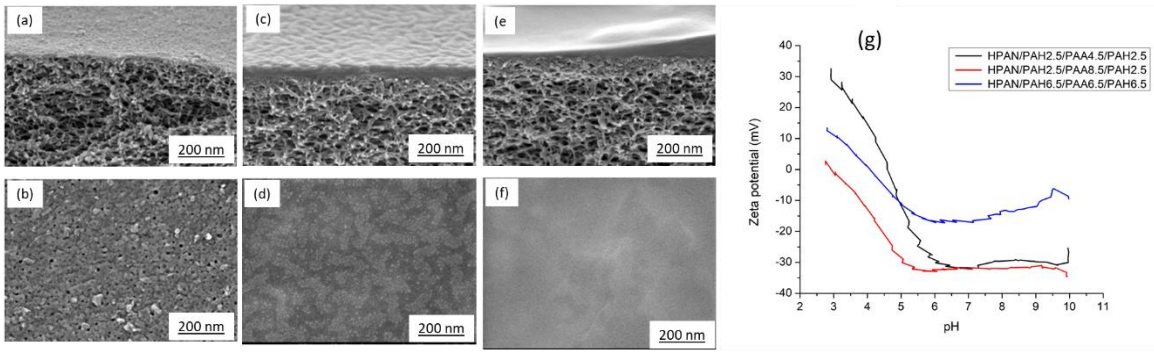

Figure 12. SEM image of PEMMs: cross section (a) and surface (b) of HPAN/PAH2.5/PAA4.5/PAH2.5, cross section (c) and surface (d) of (HPAN/PAH2.5/PAA8.5/ PAH2.5, cross section (e) and surface (f) of (HPAN/PAH6.5/PAA6.5/ PAH6.5, and Zeta potential (g) of all membranes prepared from 0.15 wt. % PE in 5mM NaCl salt solution.

4.2.4 Fourth layer deposition

Finally, the membrane was modified with PAA terminal layer using PAA solutions of pH (4.5, 6,5 and 8.5) to produce a PEMM with 2 bilayer. The membrane surface roughness continued to increase but high roughness was observed in HPAN/PAH2.5/PAA4.5/PAH2.5/PAA4.5 membrane, which is in agreement with zeta potential result where this membrane demonstrated higher negative surface charge than the other membrane in the whole pH scan range [Figure 13 (e)]. The zeta potential of all (PAH/PAA)4 membranes demonstrated a total negative ζ throughout the whole pH range of 2.5 – 10 without isoelectric point, indicating the presence of acidic groups in PAA and their corresponding dissociation into (—COO−) or –COOH. The membrane thickness increase was notable after the deposition of the fourth layer.

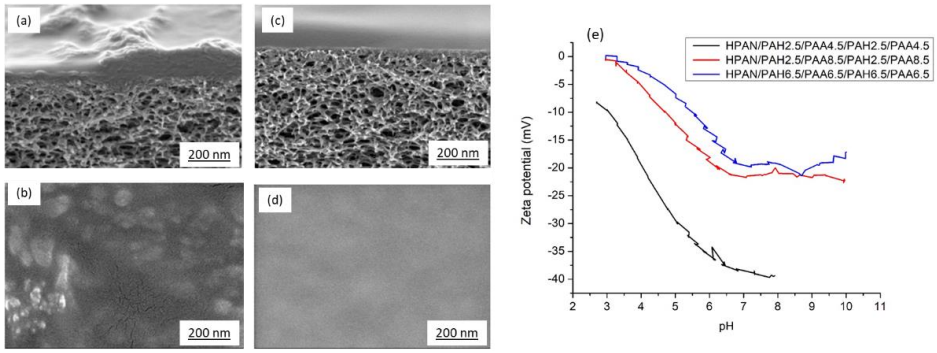

Figure 13. SEM image of PEMMs: cross section (a) and surface (b) of HPAN/PAH2.5/PAA4.5/PAH2.5/PAA4.5, cross section (c) and surface (d) of PAH6.5/PAA6.5/ PAH6.5/PAA6.5, and Zeta potential (e) of both membranes prepared from 0.15 wt. % PE in 5mM NaCl salt solution.

Generally, the SEM images collectively indicate that deposition of layered polyelectrolyte films is a simple means of creating ultrathin membranes on porous supports. Notably**,** pores of the porous membrane were still visible even after the deposition four layers indicating the majority of film coating was occurred at the support surface**.** Here, it should be noted that the lack of reproducibility observed in the SEM images could be due to the small experimental variations occurred while coating large membrane area. Furthermore, the membranes with PAA terminal layer displayed a total negative ζ throughout the whole pH range of 2.5 – 10 without isoelectric point, indicating the presence of acidic groups in PAA and their corresponding dissociation into (—COO−) or –COOH. On the contrary, PEMMs with PAH demonstrated an isoelectric point as their zeta potential shifts to positive value ascribed to the dissociation of positive groups of PAH at lower pH values. The alternating surface charge at lower pH confirms the formation of polyelectrolyte multilayer as due to the sequential deposition of oppositely charged PEs. In addition, contact angle measurement

results revealed the existence of odd-even effect i.e. PEMM showed capping layer dependent hydrophilicity characteristics. As can be seen from Figure 16, PEMMs with PAA terminal layers possessed higher hydrophilicity than the positively (PAA) terminated membranes. Thus, more hydrophilic membranes can be prepared by adjusting the pH of the coating solution and terminating the film structure with PAA outermost laye[100,102,103].

4.3 Membrane separation performance

4.3.1 Water Peremeance

Pure water permeance experiment of the virgin, hydrolyzed, and PAH/PAA modified membranes was conducted to further evaluate if the PEMs are being deposited. The water permeance ($L \cdot m^{-2} \cdot h^{-1} \cdot bar^{-1}$) of all membranes as a function of number of deposited layers is provided in (Table 1). It is clear that the hydrolyzed HPAN membrane demonstrated relatively higher water permeance than the non-modified PAN. As confirmed by the SEM images no significant morphological change has occurred to the PAN membrane after hydrolysis with NaOH solution. Hence, this higher water permeance in HPAN is attributed to the introduction of polar hydrophilic carboxyl surface groups after hydrolysis.

The water permeance of all PEMMs decreased with the number of PE layers deposited as anticipated due to an increase in the total membrane thickness as confirmed by SEM analysis (see cross-section images above). Multilayer membranes prepared from pH (6.5/6.5) exhibited the lowest water permeance. This indicates the formation of a thin and highly dense layer owing to the high ionization degree of both PEs at this pH (6.5/6.5) combination. A similar trend was observed for pure isopropyl alcohol permeance where 7 bilayers (PAH/PAA) assembled from [7.5/7.5] solution pH exhibited much lower permeance than the other membranes despite being 8-6 times thinner than the [7.5/3.5] and [3.5/3.5] membranes, respectively[54]. On the other hand, (PAH2.5/PAA8.5) membranes displayed higher pure water permeance than (PAH6.5/PAA6.5)2 indicating that the coating formed thin and less dense films.

On the other hand, the (PAH2.5/PAA4.5) membrane exhibited the highest water permeance than the other two membranes at a corresponding number of layers. This result indicates the formation of a thick and loopy or open film structure at this pH combination, which is in agreement with the

SEM results. Another significant piece of information here is, PAH2.5/PAA8.5 membrane formed highly dense film after coating with the third PAH layer as demonstrated by its pure water permeance decrease from 108.76 to 49.99, while the PAH2.5/PAA4.5 demonstrated a relatively lower decrease (75.53 to 50.41) which is mainly due to the increase in membrane resistance as a function of film thickness.

Table 1. Pure water peremeance of PEMMs ($L \cdot m^{-2} \cdot h^{-1} \cdot bar^{-1}$)

PEMM	**Pure water permeance ($L \cdot m^{-2} \cdot h^{-1} \cdot bar^{-1}$)**
PAN	282.9
HPAN	325.78
HPAN/PAH2.5	229.8
HPAN/PAH6.5	178.89
HPAN/PAH2.5/PAA4.5	75.53
HPAN/PAH2.5/PAA8.5	108.76
HPAN/PAH6.5/PAA6.5	20.68
HPAN/PAH2.5/PAA4.5/ PAH2.5	50.41
HPAN/PAH2.5/PAA8.5/ PAH2.5	49.99
HPAN/PAH6.5/PAA6.5/ PAH6.5	17.18
HPAN/PAH2.5/PAA4.5/ PAH2.5/PAH4.5	35.2
HPAN/PAH2.5/PAA8.5/ PAH2.5/PAH8.5	8.72
HPAN/PAH6.5/PAA6.5/ PAH6.5/PAH6.5	2.34

4.3.2 Gas separation performance

As mentioned in the introduction advanced membrane separations are needed for gas separation applications. Specifically, the recovery and separation of critical materials such as light olefin gas from their paraffin mixture is considered as one of the seven important chemical separation processes believed to change the word[104]. It is apparent that light olefins such as ethylene and propylene are critically needed raw materials in the chemical and petroleum industry for the production of numerous products and chemicals. However, olefins are mainly produced as olefin/paraffin mixture which demands an advanced separation process. Besides, the separation of olefin/paraffin mixture containing the same carbon number is a grand challenge and the currently used purification techniques accounts for 0.3% of global energy consumption[105]. This is because these gases have similar physical and properties such as boiling point and kinetic diameter ([105–107]. On the other hand, olefin has a double bond unlike paraffin which possess single bond. This chemical difference offers the opportunity to be exploited in olefin/paraffin separation. With this regard, these gas were selected to characterize the buildup process of PEMMs.

The pure gas permeance of ethane, ethylene, propane, propylene, and methane gases for the selected PEMMs as functions of both number of layers and pH of the coating solution is available in [Table 4. appendix]. It can be seen that at the same number of layers all gases had nearly equal permeance within the limits error. Besides, the permeance of all gases was decreasing with the number of deposited PE layers signifying the gradual sealing of the pores of the HPAN support membrane. Especially, up on the deposition of the second layer the permeance of all gases decreased rapidly, indicating complete surface coverage. There was no clear trend between the gas permeance and pH of the coating solution, except the lower permeance detected in HPAN/PAH6.5 and HPAN/PAH6.5/PAA6.5 which indicates the formation of dense film at this pH combination as witnessed in pure water permeance result.

Furthermore, the membranes displayed no selectivity towards any of the target gas since both olefin and paraffin gases had nearly equal permeance in membranes with similar number of layers. It should be noted that after the deposition of the second layer, paraffin had higher permeation than the corresponding olefin in all membranes except (PAH6.5/PAA6.5)2. The result suggest that no interaction is happening between the polymer and the double bond of olefin. According to solution diffusion model, the gas permeance is a product of diffusion and solubility coefficients. Hence, the permeation of gzases through the multilayer films is mainly dependent on the solubility of the gas molecules in the film as a function of their degree of condensability. Ethane and propane had higher permeance than ethylene propene respectively, mainly due to their higher solubility owing to their higher molecular size, critical temperature, and the boiling temperature[108] [Table 3 in appendix].

There are no much available literatures dedicated to the PEMMs based olefin/paraffin separation. Most of the works are focused on facilitated transport. Nonetheless, few attempts have been done to optimize the CO_2/N_2[109,110] by coating at higher number of bilayers which in turn cause a substantial decrease in permeance. Generally, the gas permeation results confirm the formation of multilayer membrane structure where denser film were prepared from PE pairs containing a fully charged chains.

Table 2. Ideal selectivity of all gases through the selected PEMMs at 23 °C, 1 bar feed pressure and permeate pressure increase between 1-10 mbar.

PEMM	Ideal selectivity				
	C_2H_6/C_2H_4	C_3H_8/C_3H_6	CH_4/C_3H_8	CH_4/C_3H_6	CH_4/C_2H_6
PAN	0.90	1.04	1.41	1.46	1.4
HPAN	0.98	0.97	1.92	1.86	1.67
HPAN/PAH2.5	1.01	1.03	1.27	1.31	1.2
HPAN/PAH6.5	1.55	1.53	0.70	1.07	0.84
HPAN/PAH2.5/PAA4.5	0.98	1.8	1.08	1.93	1.36
HPAN/PAH2.5/PAA8.5	1.2	1.09	1.10	1.21	1.07
HPAN/PAH6.5/PAA6.5	1.32	1.23	1.30	1.59	1.4
HPAN/PAH2.5/PAA4.5/ PAH2.5	1.35	1.3	0.99	1.28	1.064
HPAN/PAH2.5/PAA8.5/ PAH2.5	1	1.13	0.13	0.14	0.125
HPAN/PAH6.5/PAA6.5/ PAH6.5	1.48	1.45	1.63	2.364	1.46
HPAN/PAH2.5/PAA4.5/ PAH2.5/PAH4.5	1.57	1.38	2.13	2.93	1.81

5. Conclusion and recommendation

5.1. Conclusion

In conclusion, a series of polyelectrolyte multilayer membranes were prepared via layer-by-layer assembly of week polyelectrolytes (PAH and PAA) using a laboratory scale dip coating machine. The pristine microporous PAN membrane was first chemically modified using NaOH hydrolysis to get optimum conditions for creating good adhesion of the first layer. Next, the HPAN was coated with PAH and PAA while adjusting the assembly pH to control the structural and separation properties of the resulting membranes. Best surface coverage was obtained at pH combinations of 6.5/6.5 where both PEs are nearly equally charged and attained stretched conformation to fully cover the substrate surface. On the other hand, good surface coverage with detectable surface coverage was obtained at pH combinations of 2.5/8.5. On the contrary, a loose or open structure was formed at pH 2.5/4.5

Zeta potential and contact angle measurement also revealed pH-dependent surface properties which could be helpful for designing application-oriented functional membranes. Furthermore, capping layer-dependent surface properties were observed from both Zeta potential and contact angle measurements, which opens another window for controlling the properties of the multilayer membrane. SEM image

revealed an increase in membrane surface roughness with an increase in the number of deposited layers.

Finally, among the three pH combinations investigated, the 6.6/6.5 pH produced a dense film structure as backed by its water permeance result. Similarly, a thin film was formed using a 2.5/8.5 pH solution. On the contrary loose or open structure was formed at pH 2.5/4.5. Furthermore, the pure water permeance of the membranes decreased as the number of layers was increased. A similar trend was observed during a single gas permeance experiment. Nonetheless, poor gas separation performance was reported for all membranes. These results reveal that PEMMs can be suitably adjusted for use in water treatment applications ranging from dense to loose nanofiltration membranes. Hence, from this study, we can conclude that layer by layer assembly of polyelectrolytes could be a feasible way to produce functional membranes with controlled properties for use in water treatment applications

5.2 Recommendation

In this master thesis work, PEMM with four layers were prepared were prepared by systematically controlling their . It is apparent that uniformly thin and dense PEMMs was fabricated from PAH and PAA solutions pH of 6.5/6.5. Hence, it is anticipated that this membrnae could be used in various separation applications such as ion selective nanoflitration since it conatins thin selctive layer decorated with surface charge. On the contrary, the gas separation performance of PEEMs is very limited, hence, detail investigation of the interaction between polyelectrolyte multilayer and gas molecules is required.

Moreover, in a practical scenario, waste streams contain different environmnetal condition than the solution from which PEMMs are assembled, the water permance performance of these membranece in feed conatoning various acidic or basic costitutents shoud be invetigated. In addition, the effect of other parameters condition such as concentration, type of PE and ionic stregth of coating solution on the multilayer build growth process and overall separation performance should be comprehensively scrutinized in order to use this membrane in large scale application.

6. Refernce

1. UNICEF. Water Security for All. 7–7 (2021).
2. University, U. N. & Institute for Water, E. and H. GLOBAL WATER CRISIS: THE FACTS. 99–117 (1390).
3. Giljum, S., Dittrich, M., Lieber, M. & Lutter, S. Global patterns of material flows and their socio-economic and environmental implications: A MFA study on all Countries world-wide from 1980 to 2009. *Resources* **3**, 319–339 (2014).
4. Yusuf, A. *et al.* A review of emerging trends in membrane science and technology for sustainable water treatment. *Journal of Cleaner Production* vol. 266 121867 (2020).
5. Ezugbe, E. O. & Rathilal, S. membranes Membrane Technologies in Wastewater Treatment: A Review. doi:10.3390/membranes10050089.
6. Landsman, M. R. *et al.* Water treatment: Are membranes the panacea? *Annu. Rev. Chem. Biomol. Eng.* **11**, (2020).
7. Wang, D. *et al.* A general way to transform Ti3C2Tx MXene into solvent-free fluids for filler phase applications. *Chem. Eng. J.* **409**, (2021).
8. Ulbricht, M. Advanced functional polymer membranes. *Polymer* vol. 47 2217–2262 (2006).
9. Robeson, L. M. Correlation of separation factor versus permeability for polymeric membranes. *J. Memb. Sci.* **62**, 165–185 (1991).
10. Bernardo, P., Drioli, E. & Golemme, G. Membrane gas separation: A review/state of the art. *Ind. Eng. Chem. Res.* **48**, 4638–4663 (2009).
11. Baker, R. W. *Membrane Technology and Applications*. *Membrane Technology and Applications* (2012). doi:10.1002/9781118359686.
12. Zhao, Q., An, Q. F., Ji, Y., Qian, J. & Gao, C. Polyelectrolyte complex membranes for pervaporation, nanofiltration and fuel cell applications. *Journal of Membrane Science* vol. 379 19–45 (2011).
13. Baker, R. W. Research needs in the membrane separation industry: Looking back, looking forward. *J. Memb. Sci.* **362**, 134–136 (2010).
14. Koros, W. J. Evolving Beyond the Thermal Age of Separation Processes: Membranes Can Lead the Way. (2004) doi:10.1002/aic.10330.
15. Yong, W. F. & Zhang, H. Recent advances in polymer blend membranes for gas separation

and pervaporation. *Progress in Materials Science* vol. 116 100713 (2021).

16. Adewole, J. K., Ahmad, A. L., Ismail, S. & Leo, C. P. Current challenges in membrane separation of CO2 from natural gas: A review. *International Journal of Greenhouse Gas Control* vol. 17 46–65 (2013).
17. Erik, M., Sillanpää, T., Ma, X. & Shao, L. Article 3 Citation: Shao L (2020) Grand Challenges in Emerging Separation Technologies. Front. *Front. Environ. Chem.* | *www.frontiersin.org* **1**, 3 (2020).
18. Su, Y. Chapter 1: Current State-of-the-art Membrane Based Filtration and Separation Technologies. in *RSC Nanoscience and Nanotechnology* vols 2019-Janua 1–13 (2019).
19. Hermans, S., Mariën, H., Van Goethem, C. & Vankelecom, I. F. Recent developments in thin film (nano)composite membranes for solvent resistant nanofiltration. *Current Opinion in Chemical Engineering* vol. 8 45–54 (2015).
20. Cheng, W. *et al.* Selective removal of divalent cations by polyelectrolyte multilayer nanofiltration membrane: Role of polyelectrolyte charge, ion size, and ionic strength. *J. Memb. Sci.* **559**, 98–106 (2018).
21. Yan, C., Zhang, S., Yang, D. & Jian, X. Preparation and Characterization of Chloromethylated/ Quaternized Poly(phthalazinone ether sulfone ketone) for Positively Charged Nanofiltration Membranes. *J Appl Polym Sci* **107**, 1809–1816 (2007).
22. Yan, C. *et al.* Preparation, Morphologies, and Properties of Positively Charged Quaternized Poly(phthalazinone ether sulfone ketone) Nanofiltration Membranes. *J Appl Polym Sci* **113**, 1389–1397 (2009).
23. Wang, H., Zhang, Q. & Zhang, S. Positively charged nanofiltration membrane formed by interfacial polymerization of 3,3',5,5'-biphenyl tetraacyl chloride and piperazine on a poly(acrylonitrile) (PAN) support. *J. Memb. Sci.* **378**, 243–249 (2011).
24. Du, R., Chakma, A. & Feng, X. Interfacially formed poly(N,N-dimethylaminoethyl methacrylate)/polysulfone composite membranes for CO2/N2 separation. *J. Memb. Sci.* **290**, 19–28 (2007).
25. Lianchao, L., Baoguo, W., Huimin, T., Tianlu, C. & Jiping, X. A novel nanofiltration membrane prepared with PAMAM and TMC by in situ interfacial polymerization on PEK-C ultrafiltration membrane. *J. Memb. Sci.* **269**, 84–93 (2006).
26. Zhong, P. S., Widjojo, N., Chung, T. S., Weber, M. & Maletzko, C. Positively charged

nanofiltration (NF) membranes via UV grafting on sulfonated polyphenylenesulfone (sPPSU) for effective removal of textile dyes from wastewater. *J. Memb. Sci.* **417**–**418**, 52–60 (2012).

27. Deng, H., Xu, Y., Chen, Q., Wei, X. & Zhu, B. High flux positively charged nanofiltration membranes prepared by UV-initiated graft polymerization of methacrylatoethyl trimethyl ammonium chloride (DMC) onto polysulfone membranes. *J. Memb. Sci.* **366**, 363–372 (2011).
28. Yamaguchi, T., Nakao, S. I. & Kimura, S. Plasma-Graft Filling Polymerization: Preparation of a New Type of Pervaporation Membrane for Organic Liquid Mixtures. *Macromolecules* **24**, 5522–5527 (1991).
29. Bonekamp, B. C., Kreiter, R. & Vente, J. F. Sol-Gel Approaches in the Synthesis of Membrane Materials for Nanofiltration and Pervaporation. in 47–65 (2008). doi:10.1007/978-1-4020-8514-7_3.
30. Abtahi, S. M. *et al.* Micropollutant rejection of annealed polyelectrolyte multilayer based nanofiltration membranes for treatment of conventionally-treated municipal wastewater. *Sep. Purif. Technol.* **209**, 470–481 (2019).
31. Li, X., Liu, C. & Van Der Bruggen, B. Polyelectrolytes self-Assembly: Versatile membrane fabrication strategy. *Journal of Materials Chemistry A* vol. 8 20870–20896 (2020).
32. Decher, G. & Hong, J. -D. Buildup of ultrathin multilayer films by a self-assembly process, 1 consecutive adsorption of anionic and cationic bipolar amphiphiles on charged surfaces. *Makromol. Chemie. Macromol. Symp.* **46**, 321–327 (1991).
33. Michel, M., Toniazzo, V., Ruch, D. & Ball, V. Deposition Mechanisms in Layer-by-Layer or Step-by-Step Deposition Methods: From Elastic and Impermeable Films to Soft Membranes with Ion Exchange Properties. *ISRN Mater. Sci.* **2012**, 1–13 (2012).
34. Ariga, K., Hill, J. P. & Ji, Q. Layer-by-layer assembly as a versatile bottom-up nanofabrication technique for exploratory research and realistic application. doi:10.1039/b700410a.
35. Stumme, J., Ashokkumar, O., Dillmann, S., Niestroj-Pahl, R. & Ernst, M. Theoretical evaluation of polyelectrolyte layering during layer-by-layer coating of ultrafiltration hollow fiber membranes. *Membranes (Basel).* **11**, 1–18 (2021).
36. Guzmán, E. *et al.* Adsorption kinetics and mechanical properties of Ultrathin

polyelectrolyte multilayers: Liquid-supported versus solid-supported films. *J. Phys. Chem. B* **113**, 7128–7137 (2009).

37. Schlenoff, J. B. & Dubas, S. T. Mechanism of polyelectrolyte multilayer growth: Charge overcompensation and distribution. *Macromolecules* **34**, 592–598 (2001).
38. Joseph, N., Ahmadiannamini, P., Hoogenboom, R. & Vankelecom, I. F. J. Layer-by-layer preparation of polyelectrolyte multilayer membranes for separation. *Polymer Chemistry* vol. 5 1817–1831 (2014).
39. Tang, Z., Wang, Y., Podsiadlo, P. & Kotov, N. A. Biomedical applications of layer-by-layer assembly: From biomimetics to tissue engineering. *Advanced Materials* vol. 18 3203–3224 (2006).
40. Rivero, P. J., Goicoechea, J. & Arregui, F. J. Layer-by-layer nano-assembly: A powerful tool for optical fiber sensing applications. *Sensors (Switzerland)* vol. 19 (2019).
41. Lutkenhaus, J. L. & Hammond, P. T. Electrochemically enabled polyelectrolyte multilayer devices: From fuel cells to sensors. *Soft Matter* **3**, 804–816 (2007).
42. Joseph, N., Ahmadiannamini, P., Hoogenboom, R. & Vankelecom, I. F. J. Layer-by-layer preparation of polyelectrolyte multilayer membranes for separation. *Polymer Chemistry* vol. 5 1817–1831 (2014).
43. Zhu, X. & Jun Loh, X. Layer-by-layer assemblies for antibacterial applications. *Biomaterials Science* vol. 3 1505–1518 (2015).
44. Joseph, N., Ahmadiannamini, P., Hoogenboom, R. & Vankelecom, I. F. J. Layer-by-layer preparation of polyelectrolyte multilayer membranes for separation. *Polym. Chem.* **5**, 1817–1831 (2014).
45. Ng, L. Y., Mohammad, A. W. & Ng, C. Y. A review on nanofiltration membrane fabrication and modification using polyelectrolytes: Effective ways to develop membrane selective barriers and rejection capability. *Advances in Colloid and Interface Science* vols 197–198 85–107 (2013).
46. Zhang, G., Yan, H., Ji, S. & Liu, Z. Self-assembly of polyelectrolyte multilayer pervaporation membranes by a dynamic layer-by-layer technique on a hydrolyzed polyacrylonitrile ultrafiltration membrane. *J. Memb. Sci.* **292**, 1–8 (2007).
47. Ilyas, S., English, R., Aimar, P., Lahitte, J. F. & de Vos, W. M. Preparation of multifunctional hollow fiber nanofiltration membranes by dynamic assembly of weak

polyelectrolyte multilayers. *Colloids Surfaces A Physicochem. Eng. Asp.* **533**, 286–295 (2017).

48. Avram, A. M. *et al.* Polyelectrolyte multilayer modified nanofiltration membranes for the recovery of ionic liquid from dilute aqueous solutions. *J. Appl. Polym. Sci* **134**, 45349 (2017).
49. Shi, J., Zhang, W., Su, Y. & Jiang, Z. Composite polyelectrolyte multilayer membranes for oligosaccharides nanofiltration separation. *Carbohydr. Polym.* **94**, 106–113 (2013).
50. Toutianoush, A., Jin, W., Deligöz, H. & Tieke, B. Polyelectrolyte multilayer membranes for desalination of aqueous salt solutions and seawater under reverse osmosis conditions. (2004) doi:10.1016/j.apsusc.2004.11.068.
51. Fadhillah, F., Javaid Zaidi, S. M., Khan, Z., Khaled, M. & Hammond, P. T. Reverse osmosis desalination membrane formed from weak polyelectrolytes by spin assisted layer by layer technique. *Desalin. Water Treat.* **34**, (2011).
52. Toutianoush, A., Krasemann, L. & Tieke, B. Polyelectrolyte multilayer membranes for pervaporation separation of alcohol/water mixtures. in *Colloids and Surfaces A: Physicochemical and Engineering Aspects* vols 198–200 881–889 (Elsevier, 2002).
53. Lenk, W. & Meier-Haack, J. Polyelectrolyte multilayer membranes for pervaporation separation of aqueous-organic mixtures. *Desalination* **148**, 11–16 (2002).
54. Ilyas, S. *et al.* Weak polyelectrolyte multilayers as tunable membranes for solvent resistant nanofiltration. *J. Memb. Sci.* **514**, 322–331 (2016).
55. Cheng, W. *et al.* Selective removal of divalent cations by polyelectrolyte multilayer nanofiltration membrane: Role of polyelectrolyte charge, ion size, and ionic strength. (2018) doi:10.1016/j.memsci.2018.04.052.
56. Miller, M. D. & Bruening, M. L. Correlation of the swelling and permeability of polyelectrolyte multilayer films. *Chem. Mater.* **17**, 5375–5381 (2005).
57. Wang, J., Yao, Y., Yue, Z. & Economy, J. Preparation of polyelectrolyte multilayer films consisting of sulfonated poly (ether ether ketone) alternating with selected anionic layers. *J. Memb. Sci.* **337**, 200–207 (2009).
58. Dodoo, S., Balzer, B. N., Hugel, T., Laschewsky, A. & Von Klitzing, R. André Laschewsky & Regine von Klitzing (2013) Effect of Ionic Strength and Layer Number on Swelling of Polyelectrolyte Multilayers in Water Vapour. *Soft Mater.* **11**, 157–164 (2013).

59. Schlenoff, J. B., Ly, H. & Li, M. *Charge and Mass Balance in Polyelectrolyte Multilayers*. https://pubs.acs.org/sharingguidelines (1998).
60. de Grooth, J., Oborný, R., Potreck, J., Nijmeijer, K. & de Vos, W. M. The role of ionic strength and odd-even effects on the properties of polyelectrolyte multilayer nanofiltration membranes. *J. Memb. Sci.* **475**, 311–319 (2015).
61. Patel, P. A., Dobrynin, A. V. & Mather, P. T. Combined effect of spin speed and ionic strength on polyelectrolyte spin assembly. *Langmuir* **23**, (2007).
62. Dodoo, S., Steitz, R., Laschewsky, A. & Von Klitzing, R. Effect of ionic strength and type of ions on the structure of water swollen polyelectrolyte multilayers. *Phys. Chem. Chem. Phys.* **13**, 10318–10325 (2011).
63. Dubas, S. T. & Schlenoff, J. B. Factors controlling the growth of polyelectrolyte multilayers. *Macromolecules* **32**, 8153–8160 (1999).
64. Duong, P. H. H., Zuo, J. & Chung, T. S. Highly crosslinked layer-by-layer polyelectrolyte FO membranes: Understanding effects of salt concentration and deposition time on FO performance. *J. Memb. Sci.* **427**, 411–421 (2013).
65. Antipov, A. A., Sukhorukov, G. B. & Möhwald, H. Influence of the ionic strength on the polyelectrolyte multilayers' permeability. *Langmuir* **19**, (2003).
66. Schlenoff, J. B. & Dubas, S. T. Mechanism of Polyelectrolyte Multilayer Growth: Charge Overcompensation and Distribution. (2001) doi:10.1021/ma0003093.
67. Guzm an, E., an Ritacco, H., F Rubio, J. E., on Rubio, R. G. & Ortega, F. Salt-induced changes in the growth of polyelectrolyte layers of poly(diallyl-dimethylammonium chloride) and poly(4-styrene sulfonate of sodium) †. (2009) doi:10.1039/b901193e.
68. Blomberg, E., Poptoshev, E. & Caruso, F. Surface Interactions during Polyelectrolyte Multilayer Build-Up. 2. The Effect of Ionic Strength on the Structure of Preformed Multilayers. (2006) doi:10.1021/la052946y.
69. te Brinke, E., Achterhuis, I., Reurink, D. M., de Grooth, J. & de Vos, W. M. Multiple Approaches to the Buildup of Asymmetric Polyelectrolyte Multilayer Membranes for Efficient Water Purification. *ACS Appl. Polym. Mater.* **2**, 715–724 (2020).
70. Ahmadiannamini, P., Li, X., Goyens, W., Meesschaert, B. & Vankelecom, I. F. J. Multilayered PEC nanofiltration membranes based on SPEEK/PDDA for anion separation. *J. Memb. Sci.* **360**, 250–258 (2010).

71. Schönhoff, M. Layered polyelectrolyte complexes: physics of formation and molecular properties. *J. Phys. Condens. Matter* **15**, R1781–R1808 (2003).
72. V. Klitzing, R. Internal structure of polyelectrolyte multilayer assemblies. *Physical Chemistry Chemical Physics* vol. 8 5012–5033 (2006).
73. Remmen, K. *et al.* Layer-by-layer membrane modification allows scandium recovery by nanofiltration. *Environ. Sci. Water Res. Technol.* **5**, 1683–1688 (2019).
74. Stanton, B. W., Harris, J. J., Miller, M. D. & Bruening, M. L. Ultrathin, multilayered polyelectrolyte films as nanofiltration membranes. *Langmuir* **19**, 7038–7042 (2003).
75. Ilyas, S., de Grooth, J., Nijmeijer, K. & De Vos, W. M. Multifunctional polyelectrolyte multilayers as nanofiltration membranes and as sacrificial layers for easy membrane cleaning. *J. Colloid Interface Sci.* **446**, 365–372 (2015).
76. Sanyal, O., Sommerfeld, A. N. & Lee, I. Design of ultrathin nanostructured polyelectrolyte-based membranes with high perchlorate rejection and high permeability. *Sep. Purif. Technol.* **145**, 113–119 (2015).
77. Shiratori, S. S. & Rubner, M. F. pH-dependent thickness behavior of sequentially adsorbed layers of weak polyelectrolytes. *Macromolecules* **33**, 4213–4219 (2000).
78. Magnenet, C., Jurin, F. E., Lakard, S., Buron, C. C. & Lakard, B. Polyelectrolyte modification of ultrafiltration membrane for removal of copper ions. *Colloids Surfaces A Physicochem. Eng. Asp.* **435**, 170–177 (2013).
79. Zhang, G. *et al.* Preparation of polyelectrolyte multilayer membranes by dynamic layer-by-layer process for pervaporation separation of alcohol/water mixtures. *J. Memb. Sci.* **280**, 727–733 (2006).
80. SU, B., Wang, T., Wang, Z., Gao, X. & Gao, C. Preparation and performance of dynamic layer-by-layer PDADMAC/PSS nanofiltration membrane. *J. Memb. Sci.* **423**–**424**, 324–331 (2012).
81. Ji, S., Zhang, G., Liu, Z., Peng, Y. & Wang, Z. Evaluations of polyelectrolyte multilayer membranes assembled by a dynamic layer-by-layer technique. *Desalination* **234**, 300–306 (2008).
82. Wang, J., Yue, Z., Ince, J. S. & Economy, J. Preparation of nanofiltration membranes from polyacrylonitrile ultrafiltration membranes. *J. Memb. Sci.* **286**, 333–341 (2006).
83. Kim, I. C., Yun, H. G. & Lee, K. H. Preparation of asymmetric polyacrylonitrile membrane

with small pore size by phase inversion and post-treatment process. *J. Memb. Sci.* **199**, 75–84 (2002).

84. Hsieh, M. C., Farris, R. J. & McCarthy, T. J. Surface 'priming' for layer-by-layer deposition: Polyelectrolyte multilayer formation on allylamine plasma-modified poly(tetrafluoroethylene). *Macromolecules* **30**, 8453–8458 (1997).
85. Liu, Y., Chen, G. Q., Yang, X. & Deng, H. Preparation of layer-by-layer nanofiltration membranes by dynamic deposition and crosslinking. *Membranes (Basel).* **9**, (2019).
86. Zhang, G., Meng, H. & Ji, S. Hydrolysis differences of polyacrylonitrile support membrane and its influences on polyacrylonitrile-based membrane performance. *Desalination* **242**, 313–324 (2009).
87. Joseph, N., Ahmadiannamini, P., Jishna, P. S., Volodin, A. & Vankelecom, I. F. J. 'Up-scaling' potential for polyelectrolyte multilayer membranes. *J. Memb. Sci.* **492**, 271–280 (2015).
88. Hagen, D. A., Foster, B., Stevens, B. & Grunlan, J. C. Shift-time polyelectrolyte multilayer assembly: Fast film growth and high gas barrier with fewer layers by adjusting deposition time. *ACS Macro Lett.* **3**, 663–666 (2014).
89. Klingberg, P., Wilkner, K., Schlüter, M., Grünauer, J. & Shishatskiy, S. Separation of carbon dioxide from real power plant flue gases by gas permeation using a supported ionic liquid membrane: An investigation of membrane stability. *Membranes (Basel).* **9**, (2019).
90. Yousef, S. *et al.* A new industrial technology for mass production of graphene/peba membranes for CO2/CH4 selectivity with high dispersion, thermal and mechanical performance. *Polymers (Basel).* **12**, 831 (2020).
91. Van Der Bruggen, B. *et al.* Characteristics and performance of a 'universal' membrane suitable for gas separation, pervaporation, and nanofiltration applications. *J. Phys. Chem. B* **110**, 13799–13803 (2006).
92. Escorihuela, S. *et al.* Gas separation properties of polyimide thin films on ceramic supports for high temperature applications. *Membranes (Basel).* **8**, (2018).
93. Qin, Y., Yang, H., Xu, Z. & Li, F. Surface Modification of Polyacrylonitrile Membrane by Chemical Reaction and Physical Coating: Comparison between Static and Pore-Flowing Procedures. *ACS Omega* **3**, (2018).
94. Lohokare, H. R., Kumbharkar, S. C., Bhole, Y. S. & Kharul, U. K. Surface modification of

polyacrylonitrile based ultrafiltration membrane. *J. Appl. Polym. Sci.* **101**, 4378–4385 (2006).

95. Kolasińska, M., Krastev, R. & Warszyński, P. Characteristics of polyelectrolyte multilayers: Effect of PEI anchoring layer and posttreatment after deposition. *J. Colloid Interface Sci.* **305**, 46–56 (2007).
96. Wang, X. P. Preparation of crosslinked alginate composite membrane for dehydration of ethanol-water mixtures. *J. Appl. Polym. Sci.* **77**, 3054–3061 (2000).
97. Jin, S. Y., Kim, M. H., Jeong, Y. G., Yoon, Y. Il & Park, W. H. Effect of alkaline hydrolysis on cyclization reaction of PAN nanofibers. *Mater. Des.* **124**, 69–77 (2017).
98. Pérez-Álvarez, L., Ruiz-Rubio, L., Moreno, I. & Vilas-Vilela, J. L. Characterization and optimization of the alkaline hydrolysis of polyacrylonitrile membranes. *Polymers (Basel).* **11**, (2019).
99. Silverstein, R. W. & Bassler, G. C. Spectrometric identification of organic compounds. *J. Chem. Educ.* **39**, 546–553 (1962).
100. Ilyas, S., Abtahi, S. M., Akkilic, N., Roesink, H. D. W. & de Vos, W. M. Weak polyelectrolyte multilayers as tunable separation layers for micro-pollutant removal by hollow fiber nanofiltration membranes. *J. Memb. Sci.* **537**, 220–228 (2017).
101. Tripathi, B. P., Dubey, N. C. & Stamm, M. Functional polyelectrolyte multilayer membranes for water purification applications. *J. Hazard. Mater.* **252**–**253**, 401–412 (2013).
102. Elzbieciak, M., Kolasinska, M. & Warszynski, P. Characteristics of polyelectrolyte multilayers: The effect of polyion charge on thickness and wetting properties. *Colloids Surfaces A Physicochem. Eng. Asp.* **321**, 258–261 (2008).
103. Yoo, D., Shiratori, S. S. & Rubner, M. F. Controlling bilayer composition and surface wettability of sequentially adsorbed multilayers of weak polyelectrolytes. *Macromolecules* **31**, (1998).
104. Sholl, D. S. & Lively, R. P. Seven chemical separations to change the world. *Nature* vol. 532 435–437 (2016).
105. Ren, Y. *et al.* Membrane-Based Olefin/Paraffin Separations. *Advanced Science* vol. 7 (2020).
106. Faiz, R. & Li, K. Olefin/paraffin separation using membrane based facilitated

transport/chemical absorption techniques. *Chemical Engineering Science* vol. 73 261–284 (2012).

107. Hou, J. *et al.* Olefin/paraffin separation through membranes: From mechanisms to critical materials. *Journal of Materials Chemistry A* vol. 7 (2019).
108. Davoodi, S. M., Sadeghi, M., Naghsh, M. & Moheb, A. Olefin-paraffin separation performance of polyimide Matrimid®/silica nanocomposite membranes. *RSC Adv.* **6**, 23746–23759 (2016).
109. Stroeve, P., Vasquez, V., Coelho, M. A. N. & Rabolt, J. F. Gas transfer in supported films made by molecular self-assembly of ionic polymers. *Thin Solid Films* **284**–**285**, 708–712 (1996).
110. Leväsalmi, J. M. & McCarthy, T. J. Poly(4-methyl-1-pentene)-supported polyelectrolyte multilayer films: Preparation and gas permeability. *Macromolecules* **30**, 1752–1757 (1997).
111. Ren, Y. *et al.* Membrane-Based Olefin/Paraffin Separations. (2020) doi:10.1002/advs.202001398.

7. Appendix

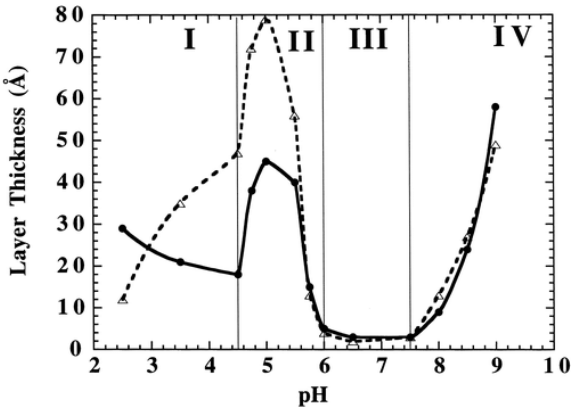

Figure 14. Average incremental thickness contributed by a PAA and PAH adsorbed layer as function of solution pH. Both the PAH and PAA dipping solutions in this case were at the same pH. Solid line represents the PAA layer thickness, and the dashed line is the PAH[77].

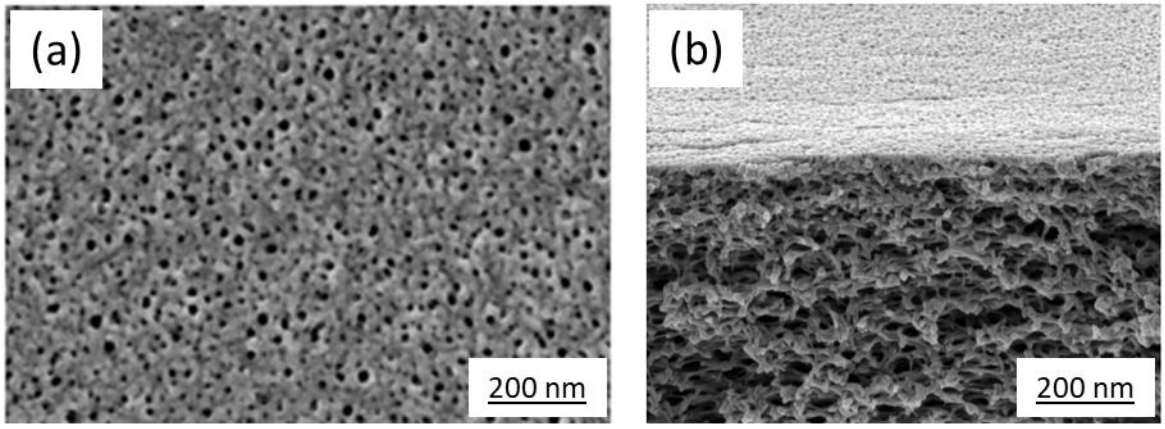

Figure 15. SEM (a) surface and (b) cross section image of HPAN hydrolyzed under 2M NaOH solution and hydrolysis time of 2 hours.

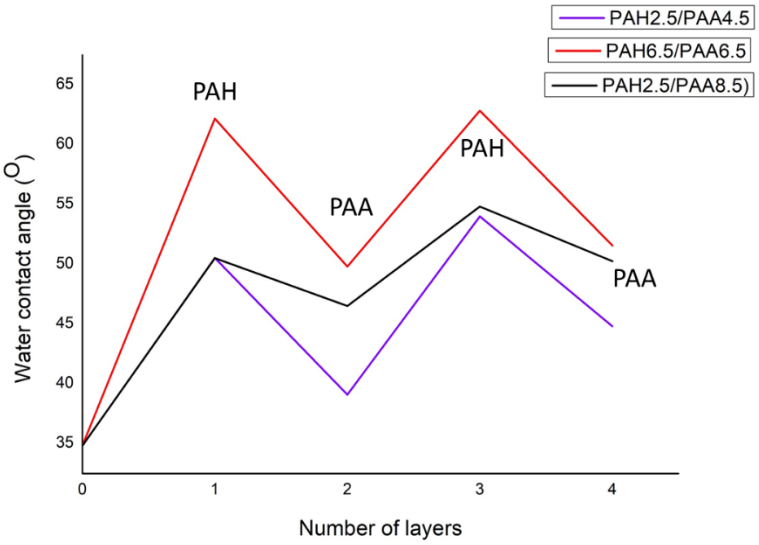

Figure 16. Water contact angle measurement of selected PEMMs prepared from different pH combinations as a function of bilayer

Table 3. Physical properties of Ethylene, Ethane, Propylene and Propane gases[111]

Component	**Boiling point [K]**	**Critical temperature [K]**	**Kinetic diameter [nm]**	**Polarizability 10^{25} [cm]**	**Dipole moment 10^{18} [esu cm]**
Ethylene	169.5	282.3	0.423	42.5	0
Ethane	184.5	305.3	0.442	44.3	0
Propylene	225.5	364.9	0.468	62.6	0.366
Propane	231.1	369.8	0.506	63.3	0.084

Table 4. permeance of all gases through the selected PEMMs at 23 °C, 1 bar feed pressure and permeate pressure increase between 1-10 mbar.

PEMM	Gas permeance (GPU)=[m³(stp)/(m²·h·bar)]				
	C_2H_6	**C_2H_4**	**C_3H_8**	**C_3H_6**	**CH_4**
PAN	50.75	56.18	51	49.26	71.81
HPAN	20.32	20.73	17.7	18.27	33.95
HPAN/PAH2.5	1.04	1.03	0.99	0.96	1.25

HPAN/PAH6.5	0.84	0.86	1.06	0.59	1.14
HPAN/PAH2.5/PAA4.5	1.38	0.89	1.65	1.08	1.16
HPAN/PAH2.5/PAA8.5	0.6	0.5	0.58	0.53	0.64
HPAN/PAH6.5/PAA6.5	0.69	0.51	0.74	0.57	0.73
HPAN/PAH2.5/PAA4.5/ PAH2.5	0.25	0.19	0.27	0.22	0.35
HPAN/PAH2.5/PAA8.5/ PAH2.5	0.08	0.08	0.079	0.07	0.01
HPAN/PAH6.5/PAA6.5/ PAH6.5	0.089	0.06	0.08	0.055	0.13
HPAN/PAH2.5/PAA4.5/ PAH2.5/PAH4.5	0.047	0.03	0.04	0.029	0.085